https://doi.org/10.1016/j.apenergy.2021.116733

Hybrid renewable energy applications in zero-energy buildings and communities integrating battery and hydrogen vehicle storage

Jia Liu [a*], Xi Chen [b], Hongxing Yang [a*], Kui Shan [c, a]

[a] Department of Building Services Engineering, The Hong Kong Polytechnic University, Kowloon, Hong Kong, China

[b] School of Science and Technology, The Open University of Hong Kong, Hong Kong, China

[c] Research Institute for Smart Energy, The Hong Kong Polytechnic University, Kowloon, Hong Kong, China

Abstract

This study presents hybrid renewable energy systems integrated with stationary battery and mobile hydrogen vehicle storage for a zero-energy community consisting of campus, office and residential buildings based on practical energy use data and simulations. A time-of-use grid penalty cost model evaluating grid import and export during on-peak and off-peak periods is proposed to achieve the power grid flexibility and economy. Multi-objective optimizations are conducted to size zero-energy buildings and the community considering the renewable energy self-consumption, on-site load coverage and grid penalty cost in the coupled platform of TRNSYS and jEplus+EA. The study results indicate that battery storage improves the renewable energy self-consumption, load coverage, hydrogen system efficiency and grid integration of the zero-energy community. Grid penalty cost reductions of 145.36% - 158.92% and 135.05% - 164.41% are achieved in zero-energy scenarios with and without battery storage compared with baseline scenarios without renewable energy. The lifetime net present value of four zero-energy scenarios with battery storage is increased by 22.39% - 96.17% compared with baseline scenarios, while it is reduced by 6.45% of US$ 7.62M and 1.90% of US$ 2.16M in zero-energy campus and residential buildings without battery storage. Substantial environmental benefits are also achieved in zero-energy scenarios with and without battery storage for reducing carbon emissions by 71.23% - 90.93% and 67.57% - 91.36%, respectively. Such a comprehensive techno-economic-environmental feasibility study can offer significant guidance for relative stakeholders to develop renewable energy applications for zero-energy buildings and communities in urban areas.

Keywords: Solar photovoltaic; Wind turbine; Battery storage; Hydrogen vehicle; Zero-energy community

* Corresponding author 1: jiajia.liu@connect.polyu.hk
* Corresponding author 2: hong-xing.yang@polyu.edu.hk

The short version of the paper was presented at Applied Energy Symposium: MIT A+ B, August 13-14, Boston. This paper is a substantial extension of the short version of the conference paper.

1. Introduction

1.1. Background

The building sector accounts for 30% of the global final energy use and 28% of energy-related carbon emissions in 2018 as the largest contributor, followed by the transport sector contributing 28% of the global final energy use and 23% of carbon emissions [1]. Similar high shares of carbon emissions are also observed in the building sector (over 60%) and transport sector (16%) in high-density cities like Hong Kong [2]. Therefore, the building and transport sectors should be targeted as major sources for greenhouse gas emission mitigation efforts. About 13% of the global energy use and 40% of global carbon emissions need to be reduced in the building sector between 2018 and 2040 to achieve the sustainable development scenario expected by the International Energy Agency [3]. Renewable energy is potentially adopted as a prominent solution for the building [4] and transportation sectors [5] to provide green power to buildings and electric vehicles given its sustainability [6] and environmental friendliness [7]. It is projected that all buildings must adopt renewable energy strategies by 2050 to meet net-zero energy and net-zero carbon requirements for higher local energy governance at community scales [3]. The renewable energy accounts for about 13.6% of total final energy consumption in the building sector in 2017 as the fastest growing source, while it only contributes 3.3% of total final energy consumption in the transport sector in the same year [8]. Therefore, it is significant to study renewable energy applications in large-scale zero-energy buildings and communities integrating clean transportation such as hydrogen vehicles (HVs) to accelerate renewable energy deployment in the building and transport sectors.

HVs are integrated with hybrid renewable energy systems for power supply to zero-energy buildings and communities as promising clean transportation tools considering its emerging market in the near future. Over 400 million hydrogen cars, 15 - 20 million hydrogen trucks and 5 million hydrogen buses are predicted globally by 2050 according to the Hydrogen Council [9]. The driving range of HVs can be 400 - 500 km due to the high energy density of compressed hydrogen tanks. And HVs are also attractive for the short refueling time of 3 - 5 minutes and small material footprint of fuel cells [10]. Stationary battery storage is also integrated in zero-energy buildings and communities given its high efficiency, fast response and small environmental footprint as a mature storage technology [11].

Ambitious policy and finance plans are launched globally to accelerate the clean energy transition from the fossil fuel leading market to the renewable energy leading market to reduce greenhouse gas emissions and mitigate the climate change. Specifically, nearly 10000 cities and local governments agreed to jointly reduce greenhouse gas emissions by the middle of 2019 to achieve the Paris Agreement of limiting global warming to 1.5ºC above pre-industrial levels [12]. 77 countries, ten regions and over 100 cities promised to achieve net-zero carbon emission by 2050 at the Climate Action Summit, and increasing finance supports of US$ 1.7B, US$ 100M and US$ 6M are attracted from France, Qatar and Hungary respectively [13]. A strategic roadmap is provided by the European Commission to make Europe the first carbon-neutral continent by 2050 as the frontrunner in climate-friendly industries, green technologies and green financing. It is reported that up to EUR 100B is planned for most vulnerable sectors and regions and totally EUR 260B is required to achieve the climate and energy policy targets in 2030 [14]. At least US$ 1T will be invested to support building decarbonisation in developing countries by 2030 to meet goals of the Paris Agreement under which all buildings must be net-zero carbon by 2050. However, less than 1% of buildings meet the requirement at present [15]. Significant efforts in carbon mitigation are observed in China as the world's biggest source of carbon emissions, achieving a carbon emission intensity reduction of 45% since 2005 and sharing a quarter of newly afforested lands globally [13]. Moreover, China provides an ambitious blueprint to reach the carbon emission peak before 2030 and achieve carbon neutrality before 2060 [16]. Globally, at least 57 carbon-pricing initiatives including direct taxation and trading schemes were implemented or scheduled to reduce carbon footprints in significant sectors across 47 countries covering 20% of global greenhouse gas emissions by 2019 [17].

1.2. Literature review

Hybrid renewable energy and storage applications in grid-connected building communities have drawn much attention of researchers given the power supply sustainability and increasing renewable installations. The technical, economic and environmental feasibilities of large-scale hybrid renewable energy and storage systems are investigated to provide references for relative stakeholders. And flexible solutions are also explored to improve the reliability and economy of the power grid integrated with renewable energy systems regarding the demand side control, energy storage technology, design optimization and energy policy aspects to accelerate renewable applications in urban communities.

Many types of renewable energy and storage systems have been developed to achieve sustainable power supply to building communities for technical [18], economic [19-21] and environmental [22] feasibility studies. The efficiency and economic feasibilities of using renewable hydrogen and biogas are analyzed for power and fuel supply to a 10000 resident community in California. It is shown that 80% of zero net community electricity can be fulfilled by renewable energy. The authors also report that electrolysis and solid oxide fuel cell technologies can be economically competitive with the natural gas and utility grid for community-scale energy systems in the next one or two decades [18]. A local renewable energy community is studied by developing poly-generation, electric and hydrogen storage systems for the optimal total life cycle cost. The results indicate that battery storage with a high roundtrip efficiency of 90% is more effective than power-to-gas hydrogen storage with an efficiency of 23%, while battery storage alone is not economical for community renewable energy systems [19]. Novel business models are proposed for renewable community microgrids considering the optimal sizing and energy management of the renewable energy system by minimizing the customer electricity cost. Case studies are conducted for seventeen locations in Chile with varied renewable resources and electricity tariffs, showing that community microgrids are generally more profitable than single-dwellings [20]. A 100% renewable energy network model is proposed for electrified and hydrogen cities by optimizing the total annual cost. Case studies in Korean rural and urban communities indicate that the energy carrier and energy demand structure are significant factors for the system configuration and economy [21]. The stochastic operation of multiple distributed energy systems with renewable energy is studied through a Markovian process by minimizing the expected net energy and carbon emission cost in a local energy community [22].

Research has been conducted to improve the grid integration and reliability for grid-connected large-scale renewable energy systems regarding the demand side control [23, 24], energy storage technology [25, 26], design optimization [27] and energy policy [28] aspects. Specifically, a long-term energy system optimization model is proposed to maintain the grid stability in the future French renewable application case considering flexible options such as the demand-response control, energy storage and additional plants. It is indicated that a maximum of 65% variable renewable energy can be installed to ensure the grid reliability [23]. The potential of applying combined heat and power systems in the demand side to provide the grid flexibility in variable renewable energy systems is assessed based on the case study in the greater Tokyo area.

The results show that the aggregation of different facilities effectively supports the grid flexibility [24]. Energy storage technologies such as hydrogen storage [25] and pumped hydro storage [26] are also identified to be efficient in improving the grid integration and resiliency in large-scale renewable energy applications. Multi-objective optimizations are conducted for system sizing and controlling power exchange of a grid-tied renewable energy system in an Iranian community. The study evaluates the impact of grid imported energy and grid exported energy on the system levelized cost of energy, loss of power supply probability and renewability [27]. A European dedicated transmission grid module is coupled with the POLES world energy model to improve the grid operation and flexibility under cases of large-scale variable renewable energy installations. The energy modelling framework considering the grid investment is delivered for the energy technology development and energy policy in renewable energy powered districts [28].

Research gaps can be found based on the above literature review showing that few studies have analyzed the techno-economic-environmental feasibilities of renewable energy systems in communities consisting of different building types based on real energy use data in high-density urban contexts. And community-scale renewable energy and storage systems are rarely integrated with HV groups following different schedules as both commuting tools and shared storage technologies. Furthermore, the economic performance and decarbonisation potential are seldom clarified for zero-energy buildings/communities integrating renewable energy and hydrogen transportation systems. It is also found that existing grid integration solutions mainly focus on the demand side control, energy storage technology, design optimization and energy policy aspects. Whereas business models of grid penalty cost are seldom studied considering the time-of-use electricity tariff for large-scale community applications.

1.3. Scope and contribution

To fill the above research gaps, this study develops hybrid renewable energy systems with stationary battery and hydrogen vehicle storage technologies with TRNSYS to achieve a zero-energy community including campus, office and residential building groups. A time-of-use grid penalty cost model is proposed to improve the flexibility and economy of the power grid. Multi-objective optimizations are further conducted to size zero-energy buildings and the community with a coupled modelling platform. Main contributions of this study are shown as below:

(1) Microgrid systems with shared hybrid renewable energy supply and storage are developed for a zero-energy building community consisting of campus, office and residential buildings based on actual energy use data and simulations as per local surveys and codes. Three mobile hydrogen vehicle groups following different cruise schedules are integrated as both commuting tools of building occupants and shared storage units along with stationary batteries for the community load.

(2) A time-of-use grid penalty cost business model evaluating the grid import and grid export during on-peak and off-peak periods is proposed to achieve the flexibility and economy between the renewable energy microgrid system and the utility grid. A sensitivity analysis is conducted to study the impact of the grid import estimation, grid export estimation and grid penalty factor on the time-of-use grid penalty cost.

(3) Four zero-energy scenarios of zero-energy community, zero-energy campus buildings, zero-energy office buildings and zero-energy residential buildings are developed with multi-objective optimizations to size the renewable energy and storage systems. Three optimization criteria are developed including the renewable energy self-consumption ratio, on-site load cover ratio and time-of-use grid penalty cost.

(4) The techno-economic-environmental performance of zero-energy buildings and the community with hybrid renewable energy systems integrating battery and hydrogen vehicle storage is identified compared with baseline scenarios without renewable energy. And four zero-energy scenarios without battery storage are also developed in comparison with zero-energy scenarios with battery storage and baseline scenarios to study the role of battery storage in zero-energy buildings and communities.

2. Methodology

The hybrid renewable energy and storage sharing microgrid system is developed in the TRNSYS 18 environment [29] for power supply to a zero-energy community with the overall framework shown in Fig. 1. Three typical building groups of university campus buildings as well as high-rise office and residential buildings are combined as a community with on-site collected energy use data and simulations as per local surveys and codes. The load file of the campus building group is obtained from operational data of Phase I - Phase V buildings in the Hong Kong Polytechnic University (PolyU). The load file of the office building group is collected from the commercial office zone of the International Commerce Center (ICC) in Hong Kong. And the

annual load of the high-rise residential building group is obtained from the transient simulation according to local surveys and building codes. A hybrid renewable energy system of solar photovoltaics (PV) and wind power with complementary characteristics is adopted for the shared power supply to buildings. Stationary battery units are installed in the building community serving as a shared storage among buildings. 1000 HVs in three groups following different cruise schedules are developed for the community serving both as commuting tools and shared storage. A time-of-use grid penalty cost model is proposed optimizing grid import and grid export during on-peak and off-peak periods to achieve the flexibility and economy of the power grid. An energy management strategy is also established to dynamically control the energy flow among the energy demand, hybrid supply, hybrid storage and utility grid components.

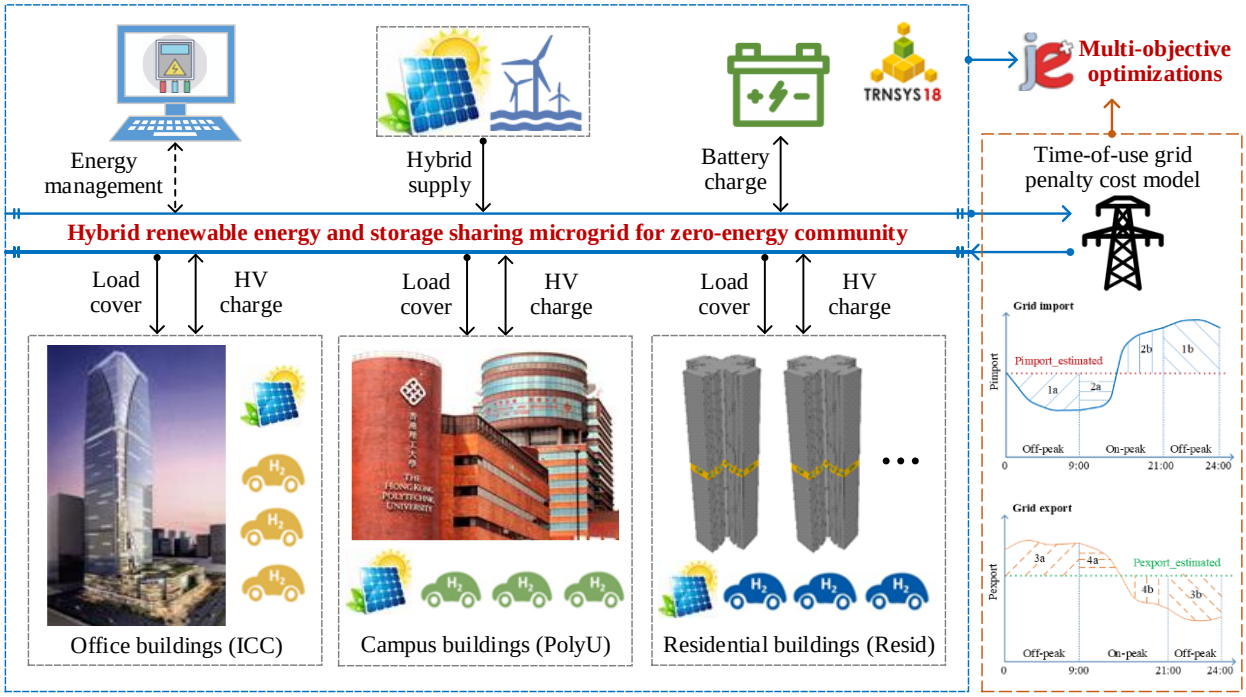

Fig. 1 Framework of hybrid renewable energy and storage system for zero-energy community

Four zero-energy scenarios are developed and optimized including the zero-energy community, zero-energy campus buildings, zero-energy office buildings and zero-energy residential buildings to compare the technical, economic and environmental performance. Multi-objective optimizations of zero-energy scenarios are conducted to determine the installation capacity of PV panels, wind turbines and battery units. Three indicators are selected as the optimization criteria including the self-consumption of renewable generation, on-site coverage of

the electrical load and time-of-use grid penalty cost. The impact of battery storage on hybrid renewable energy systems are also quantified by comparing with four zero-energy scenarios without battery storage. The energy supply, economic and decarbonisation potential performance of zero-energy scenarios is further clarified via the comparison with baseline scenarios without renewable energy supply.

2.1. Building community with three typical building groups

A typical community is established for renewable energy applications covering campus, office and residential buildings in Hong Kong based on actual energy consumption data and simulations as per local surveys and codes. The dynamic practical electricity consumption of Phase I - Phase V buildings of about 149,260 m^2 in the Hong Kong Polytechnic University (PolyU) is collected as the campus building load profile. The office building operation data is collected from the International Commerce Center (ICC) in Hong Kong. ICC is a commercial skyscraper with shopping arcades, commercial offices and hotels, but only electricity consumption of commercial offices of about 268,800 m^2 is adopted for this study. Ten typical high-rise buildings of about 192,095 m^2 in standard design layouts [30] of public residential buildings (Resid) in Hong Kong are simulated according to local on-site surveys [31] and buildings codes [32, 33] as the residential building load profile. The simulated residential building load covers the internal heat gain, air-conditioning load and domestic hot water demand, agreeing well with local survey results [34].

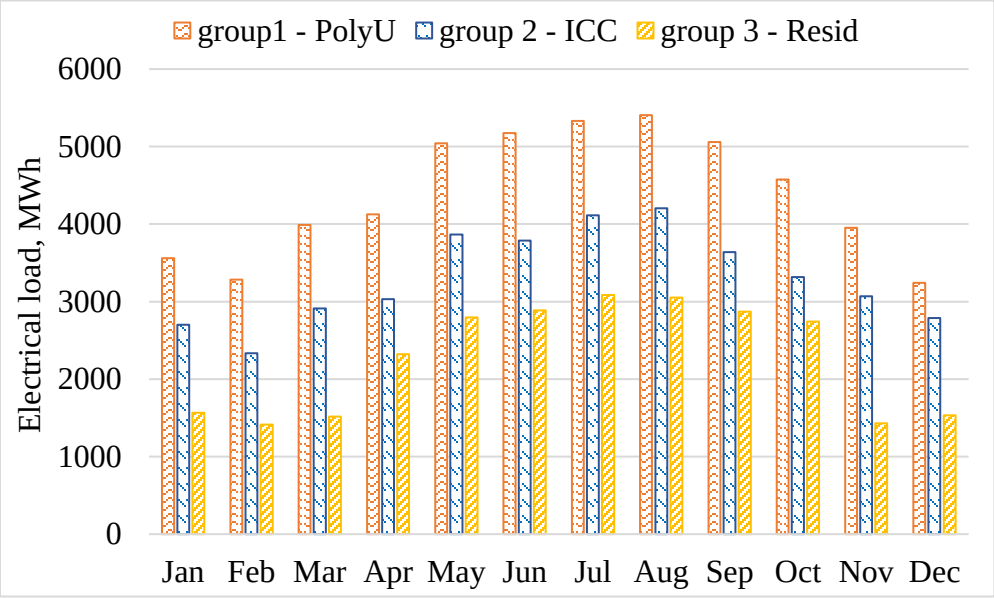

Fig. 2 Monthly electrical load of campus buildings, office buildings and residential buildings

The monthly electrical load of these three typical building groups is shown in Fig. 2. The monthly electrical load of campus buildings (group 1 - PolyU) varies between 3244 - 5406 MWh with the minimum in December and maximum in August. The minimum and maximum electrical load of office buildings (group 2 - ICC) is 2336 MWh in February and 4206 MWh in August, respectively. While the electrical load of residential buildings (group 3 - Resid) varies in the range of 1413 - 3086 MWh with the minimum in February and maximum in July. The specific annual electricity consumption of PolyU is about 353.35 kWh/m^2·year (total annual of 52740 MWh), which is higher than 147.94 kWh/m^2·year (total annual of 39767 MWh) of ICC and 141.63 kWh/m^2·year (total annual of 27206 MWh) of Resid. The total annual electrical load of the community integrating three building groups is about 119,714 MWh and the specific annual load is 196.20 kWh/m^2·year.

2.2. Hybrid renewable energy systems for zero-energy buildings and community integrating battery and hydrogen vehicle storage

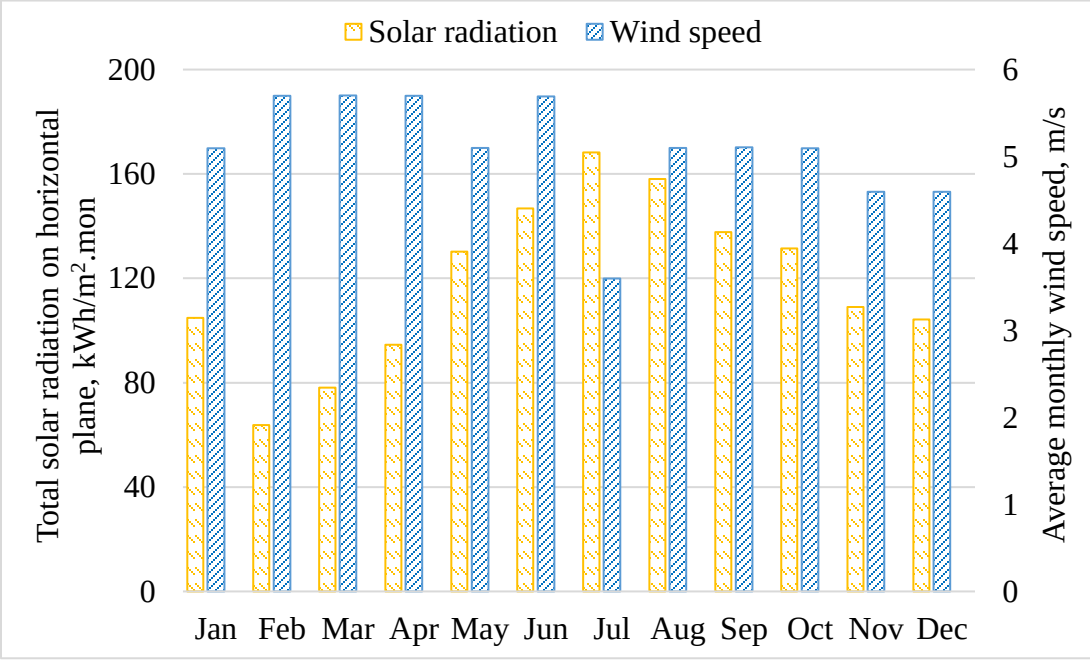

Fig. 3 Monthly solar radiation and average wind speed in Hong Kong

The monthly solar radiation and average wind speed in Hong Kong is shown in Fig. 3 based on the Meteonorm data of Hong Kong [35]. The local monthly solar radiation ranges from 63.73 - 168.22 kWh/m^2 achieving its maximum in July. The local monthly wind speed ranges from 3.60 - 5.70 m/s with an average monthly value of 5.09 m/s. It is shown that solar energy is relatively

abundant in summer while more wind energy is accessible in winter with a good seasonal complementary nature. Therefore, a hybrid solar PV and wind energy system is adopted for the three building groups and the community to achieve balanced annual renewable energy generation and annual electricity consumption.

The hybrid renewable energy and storage system for zero-energy buildings and the community is established in the TRNSYS 18 environment [29] to study the annual operational performance at a timestep of 0.125 h. The schematic of the hybrid system for the zero-energy community is shown in Fig. 4 covering the hybrid supply, stationary battery storage, mobile hydrogen vehicle storage and utility grid integration. The hybrid renewable energy supply and storage is shared in the community microgrid integrating three building groups with different schedules and load distributions.

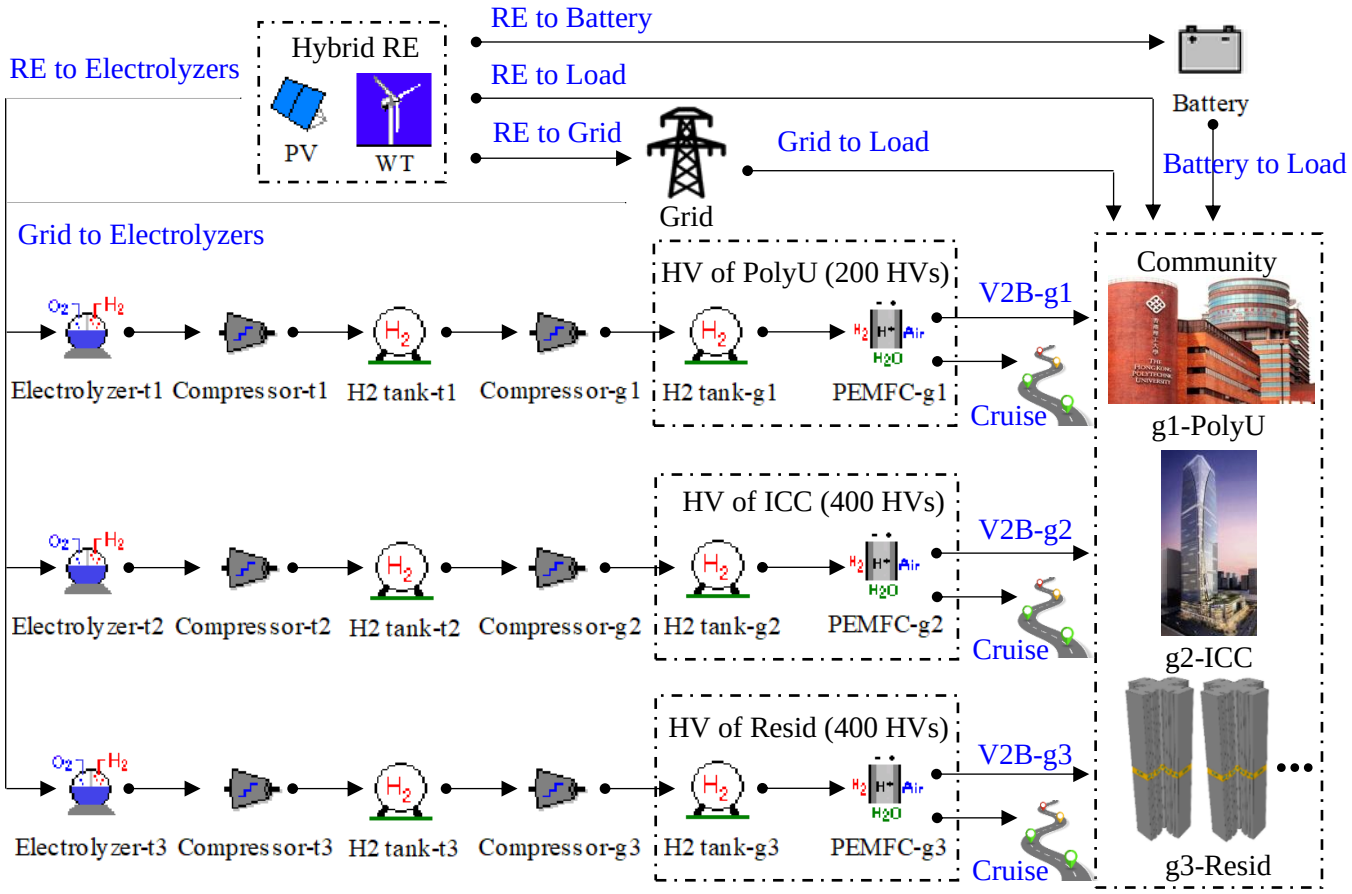

Fig. 4 Schematic of the hybrid renewable energy and storage system for zero-energy community

Hybrid renewable supply: The hybrid solar PV and wind power with complementary generation characteristics is adopted for electricity supply to the zero-energy building community.

The PV panels are simulated by TRNSYS Type 103 with the maximum power point tracked at 22º titled angle close to the latitude of the local geography. The three-blade horizontal-axis wind turbines are also installed for renewable supply modelled by Type 90 according to the tested power-speed characteristic curve of a commercialized product [36]. The installation capacity of PV panels and wind turbines are subject to multi-objective optimizations as per Section 2.4.

Battery storage: The lithium-ion batteries are installed in the building community shared by three building groups with different operational functions. Batteries can be charged by surplus renewable power or discharged to meet unsatisfied electrical load of the community. The battery charging process is controlled by the battery fractional state of charge (FSOC 0.15 - 0.98) and limited by the maximum battery charging and discharging rate (1C for the lithium-ion battery [37]) at a charging efficiency of 90% [35]. The battery capacity is determined by multi-objective optimizations and the techno-economic-environmental impact of battery storage is further investigated by comparing zero-energy scenarios with and without battery storage.

Hydrogen vehicle storage: Three groups of hydrogen vehicles (HVs) are arranged in the community according to occupants' commuting behavior of three building groups. Specifically, 200 HVs are assumed for the PolyU building group with the parking period of 10:00 - 18:00 in weekdays; 400 HVs are assumed for the ICC building group according to its car parking setting and the parking period is 9:00 - 17:00 in weekdays; 400 HVs are assumed for the Resid building group according to a local survey [38] and the parking time is 19:00 - 8:00 from Monday to Saturday and all hours in Sunday. The average daily driving distance of these vehicles is 49.25 km according to a local transport report [39]. The HV is modelled based on a commercialized product "2019 Toyota Mirai" with a full hydrogen storage of 5 kg at 700 bars and sufficient for a cruise range of up to 502 km [40]. The hydrogen consumption of three HV groups on the road is considered in the simulation by calculating the FSOC of hydrogen storage tanks of HVs. The parked HVs can also serve as shared energy storage units for the community to take in surplus renewable energy generation or be discharged for the electrical load. The utility grid is controlled to supply power to HVs when their residual hydrogen storage is not enough for daily cruise.

Each group of hydrogen system includes electrolyzers (*Electrolyzer-t*), primary compressors (*Compressor-t*) carrying hydrogen from electrolyzers to stationary hydrogen storage tanks (H_2 *tank-t*), secondary compressors (*Compressor-g*) transporting hydrogen from stationary hydrogen

storage tanks to mobile hydrogen storage tanks (*H_2 tank-g*) and proton exchange membrane fuel cells (*PEMFC-g*). The electrolyzer is simulated by Type 160a according to an alkaline electrolyzer product "PHOEBUS" [35] and the number of electrolyzer cells is determined by the power supply to keep the electrical current density within 40 - 400 mA/cm^2 [41]. The multi-stage polytropic compressor is modelled by Type 167 and external electricity is needed to drive the compressor when the entering hydrogen pressure is lower than the desired outlet pressure. The compressed hydrogen storage tank limiting to 700 bars is modelled by Type 164b based on the van der Waals equation of state for real gases [35]. Type 170d is used to simulate the electrochemical process of PEMFC converting the chemical energy of hydrogen and air to electrical currents. The generated heat accompanied by hydrogen system operations is recovered mainly from electrolyzers, compressors and fuel cells for domestic hot water applications.

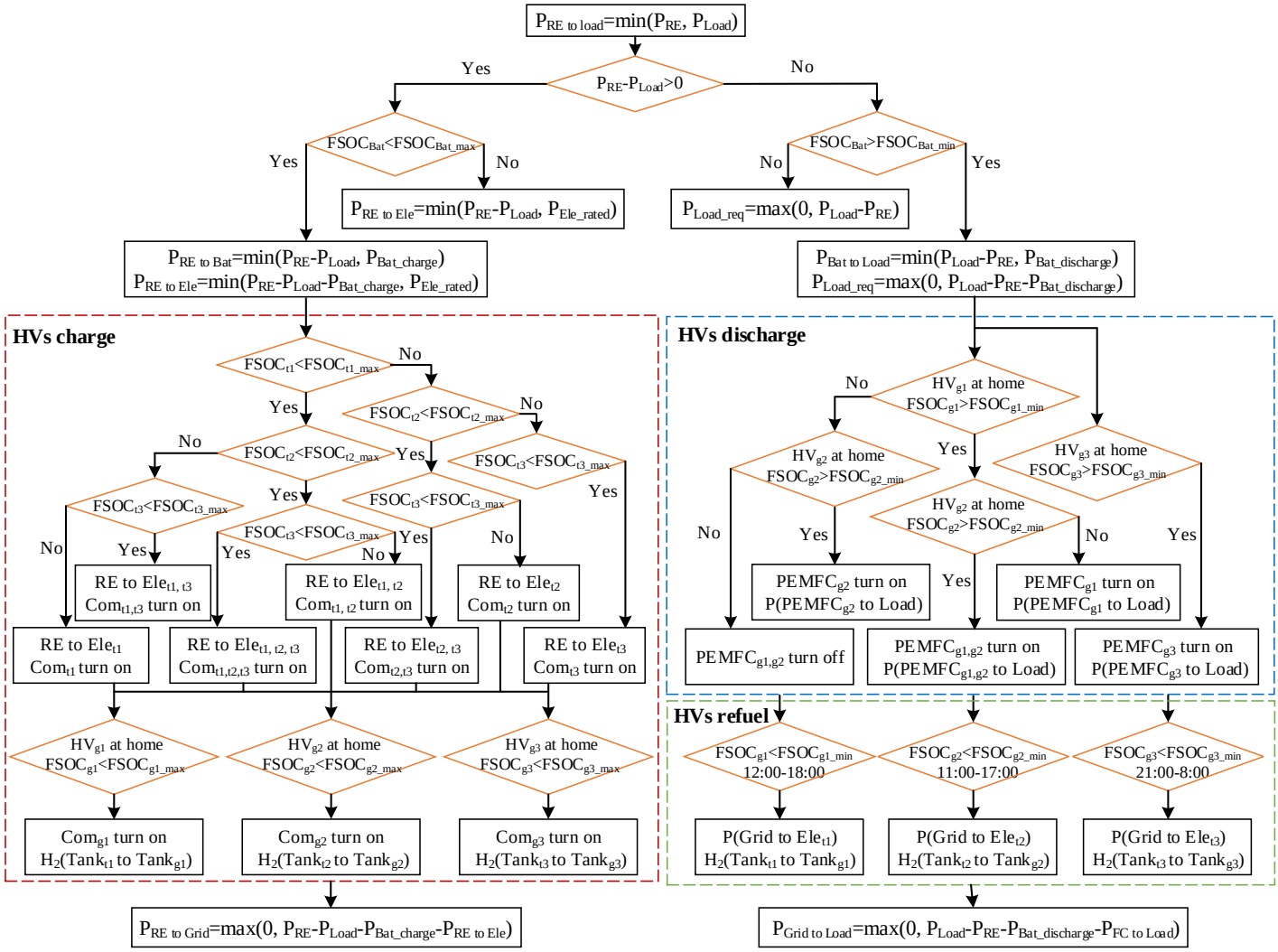

Fig. 5 Energy management strategy of renewable energy system for zero-energy community

Energy management strategy: The energy management strategy of the hybrid system integrating the stationary battery and three HV groups for the zero-energy community is shown in Fig. 5. The hybrid renewable generation power (P_{RE}) is firstly delivered to meet the electrical load (P_{Load}) of buildings. The surplus renewable energy is used to charge the stationary battery until a full state of charge ($FSOC_{Bat\_max}$ 0.98) considering the available charging capacity and charging rate limit. Then renewable energy is controlled to drive three groups of electrolyzers (Ele_t) to produce hydrogen for HVs considering the available storage state of stationary hydrogen storage tanks ($FSOC_{t\_max}$ 0.95). The corresponding primary compressors (Com_t) are turned on to transport hydrogen from electrolyzers to stationary hydrogen storage tanks ($Tank_t$) when renewable generation is supplied. And secondary compressors (Com_g) are simultaneously turned on to delivery hydrogen from stationary hydrogen storage tanks to mobile hydrogen storage tanks ($Tank_g$) when HV groups are parked at buildings controlled by its maximum storage state ($FSOC_{g\_max}$ 0.95). Finally, the residual renewable power is fed into the utility grid.

When renewable energy is not enough for electrical load of buildings, the battery unit is discharged prior to HVs considering the accessible discharging capacity ($FSOC_{Bat\_min}$ 0.15) and maximum discharging rate. Then HVs parking at buildings are controlled to consume hydrogen in PEMFCs to provide power according to the charge state of mobile storage tanks. The discharging time of parked HVs of the PolyU group and ICC group is partly overlapped (i.e. 10:00 - 17:00 in weekdays), while the discharging time of parked HVs of the Resid group is totally different with the other two groups. The minimum hydrogen level of mobile storage tanks of three HV groups ($FSOC_{g\_min}$ 0.1005) is controlled to cover one-day cruise and stay above the atmospheric pressure during the discharging process. The utility grid serves as the back up to supply power to drive electrolyzers to produce hydrogen for HVs when their storage state is lower than the minimum level. And the utility grid also supplies power for the residual unsatisfied building load.

Four zero-energy building scenarios with hybrid systems are optimized and analyzed to compare the system supply, economic and decarbonisation potential performance. ***Scenario 1***: Zero-energy community involving three typical building groups integrated with the stationary battery and three groups of HVs following different cruise schedules. The renewable supply and hybrid storage are shared in the community microgrid with three building groups in different operational functions and different load distributions. ***Scenario 2***: Zero-energy campus buildings integrated with the stationary battery and one group of HVs. ***Scenario 3***: Zero-energy office

buildings integrated with the stationary battery and one group of HVs. ***Scenario 4***: Zero-energy residential buildings integrated with the stationary battery and one group of HVs. The installation capacity of PV panels, wind turbines and batteries are optimized for each scenario by multi-objective optimizations. And four zero-energy scenarios without stationary battery storage and four baseline scenarios without renewable supply are also developed for the techno-economic-environmental performance comparison.

2.3. Time-of-use grid penalty cost model for renewable energy systems

The installation of renewable energy for power supply to buildings and communities may impose extra burden on the existing utility grid [37] especially in large-scale applications. A business model of the grid penalty cost is proposed to integrate the building community microgrid with the utility grid based on the local time-of-use electricity pricing mode counting both imported power from grid and exported power to grid. It is assumed that the on-peak period is the daily period between 9:00 and 21:00 and the off-peak period comprises all other hours according to the local power grid company [42]. The time-of-use penalty cost of renewable energy systems includes four parts, namely grid import of off-peak time and grid import of on-peak time as per Fig. 6(a), grid export of off-peak time and grid export of on-peak time as per Fig. 6(b).

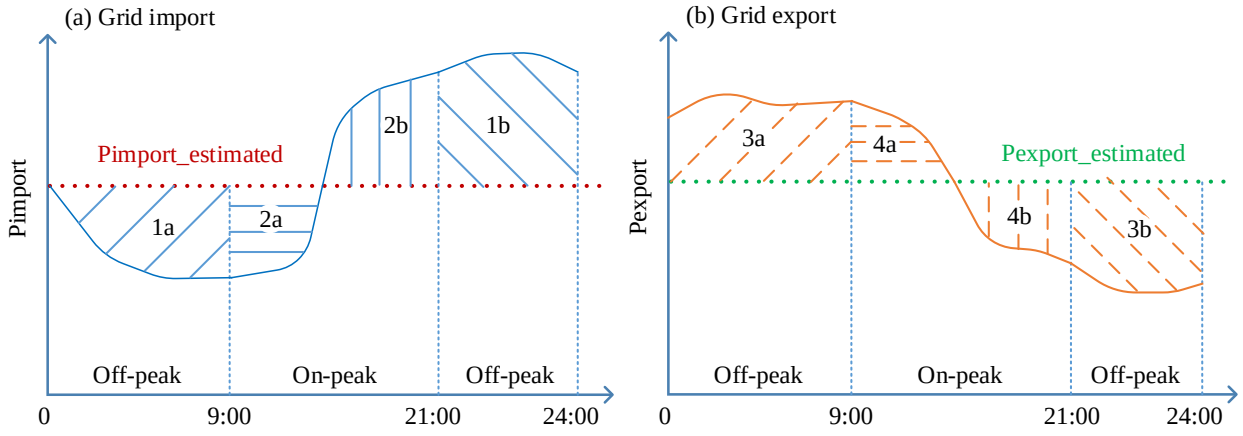

Fig. 6 Time-of-use grid penalty cost model of renewable energy systems

The formulation of penalty cost of grid import in off-peak time is shown in Eq. (1).

$$PC_{import\_offpeak}=\left(\int P_{import\_estimated}-\int P_{import\_offpeak}\right)\cdot PF_{offpeak} \quad (1)$$

where $PC_{import\_offpeak}$ is the penalty cost of imported power from grid during off-peak hours as indicated by area *1a* ($PC > 0$ with a fine when $P_{import\_offpeak} < P_{import\_estimated}$) and area *1b* ($PC < 0$ with a bonus when $P_{import\_offpeak} > P_{import\_estimated}$) in US$, as excess import is encouraged by grid during off-peak periods. $P_{import\_estimated}$ is the grid import estimation defined as the ratio of peak electrical load of buildings in kW. $P_{import\_offpeak}$ is the dynamic imported power from grid during off-peak hours, kW. $PF_{offpeak}$ is the penalty factor during off-peak hours, US$/kWh.

The formulation of penalty cost of grid import during on-peak time is shown in Eq. (2).

$$PC_{import\_onpeak} = \left(\int P_{import\_onpeak} - \int P_{import\_estimated}\right) \cdot PF_{onpeak} \tag{2}$$

where PC_{import_onpeak} is the penalty cost of imported power from grid during on-peak hours as indicated by area *2a* ($PC < 0$ when $P_{import\_onpeak} < P_{import\_estimated}$) and area *2b* ($PC > 0$ when $P_{import\_onpeak} > P_{import\_estimated}$) in US$, as extra import during on-peak periods is not preferred by grid. P_{import_onpeak} is the dynamic imported power from grid during on-peak hours, kW. PF_{onpeak} is the penalty factor during on-peak hours, US$/kWh.

The formulation of penalty cost of grid export in off-peak time is shown in Eq. (3).

$$PC_{export\_offpeak} = \left(\int P_{export\_offpeak} - \int P_{export\_estimated}\right) \cdot PF_{offpeak} \tag{3}$$

where $PC_{export\_offpeak}$ is the penalty cost of exported power from grid during off-peak hours as indicated by area *3a* ($PC > 0$ when $P_{export\_offpeak} > P_{export\_estimated}$) and area *3b* ($PC < 0$ when $P_{export\_offpeak} < P_{export\_estimated}$) in US$, as excess export in off-peak periods is not encouraged by grid. $P_{export\_offpeak}$ is the dynamic exported power to grid during off-peak hours, kW. $P_{export\_estimated}$ is the grid export estimation defined as the ratio of rated renewable energy capacity in kW.

The formulation of penalty cost of grid export in on-peak time is shown in Eq. (4).

$$PC_{export\_onpeak} = \left(\int P_{export\_estimated} - \int P_{export\_onpeak}\right) \cdot PF_{onpeak} \tag{4}$$

where PC_{export_onpeak} is the penalty cost of exported power to grid during on-peak hours as indicated by area *4a* ($PC < 0$ when $P_{export\_onpeak} > P_{export\_estimated}$) and area *4b* ($PC > 0$ when $P_{export\_onpeak} < P_{export\_estimated}$), as residual grid export is welcomed during on-peak periods. P_{export_onpeak} is the dynamic exported power from grid during on-peak hours, kW.

Therefore, the time-of-use grid penalty cost (PC_{TOU}) can be formulated as per Eq. (5):

$$PC_{TOU} = PC_{import\_offpeak} + PC_{import\_onpeak} + PC_{export\_offpeak} + PC_{export\_onpeak} \quad (5)$$

The time-of-use grid penalty cost is adopted as one of optimization criterion in multi-objective optimizations to optimize grid relief potential of zero-energy buildings and the community compared with baseline scenarios. The grid import estimation ($P_{import\_estimated}$) and grid exported estimation ($P_{export\_estimated}$) are set as 50% of the peak building load and 20% of the rated renewable capacity respectively in the optimization analysis. And a sensitivity analysis is conducted to study the impact of grid import and export estimation ratios on the total time-of-use grid penalty cost in Section 3.4. The penalty factors during off-peak time and on-peak time are defined as the ratio of the local off-peak electricity tariff and on-peak electricity tariff of imported energy from utility grid of 0.469 HK$/kWh and 0.567 HK$/kWh respectively [43]. The penalty factor ratio is also analyzed in the sensitivity analysis in Section 3.4.

2.4. Multi-objective optimization and evaluation of zero-energy buildings and community

(1) Multi-objective optimization of hybrid renewable energy systems

Multi-objective optimizations are developed to size renewable energy and storage systems for applications in zero-energy buildings and their community based on an integrated simulation platform of jEplus+EA and TRNSYS. This optimization tool has been widely used with high adaptability and flexibility integrating the integer-based encoding scheme, constrained multi-objective ranking and pareto archived global elitism [44]. Non-dominated Sorting Genetic Algorithm II (NSGA-II) is adopted given its robustness and versatility as one of the best known algorithms for multi-objective optimizations with a high efficiency in ranking competing objectives. It generates the first set of solutions with random sampling and ranks them according to the optimization criteria. Better solutions are then selected to reproduce offspring generations using a high crossover rate (0.9) and a low mutation rate (0.05) for a reasonable convergence speed and acceptable accuracy [45]. The evolution cycle ends with a set of pareto optimal solutions once the termination criteria are met. The population size is set as 10 and the maximum generation is set as 200 to ensure an exhaustive searching [46]. The minimum distance to the utopia point method is adopted to select the final optimum solution from the Pareto optimal set of the multi-objective optimizations. It identifies the optimum solution based on its distance to the utopia point, which is an ideal optimum solution supposing all objectives to be minimized simultaneously [47]. Equivalent weights are assigned to the optimization criteria in the decision-making strategy.

The installation capacities of the PV panel, wind turbine and stationary battery of four zero-energy scenarios are sized in the multi-objective optimization process. The PV capacity is dependent on the capacity of wind turbines to achieve a zero-energy building operation with balanced annual renewable energy generation and annual electricity consumption. So the capacities of wind turbine and battery are selected as the optimization variables with detailed searching range and increment shown in Table 1. The searching space of the wind turbine number is 10 - 400 with a single turbine capacity of 100 kW and the wind power generation at the maximum number almost covers all the electrical load of the community. The optimization ranges of the wind turbine number in the other three zero-energy scenarios are set according to the annual load share of the corresponding building group. The searching space of the stationary battery capacity in the zero-energy community scenario is 5000 - 75000 with the maximum capacity comparable to the storage capacity of HVs. And the search ranges of the other three scenarios are determined according to their HV number.

Table 1 Optimization variables of zero-energy buildings and community systems

Optimization variables	Wind turbine number		Battery capacity, kWh	
	Range	Increment	Range	Increment
Zero-energy community	10 - 400	10	5000 - 75000	2000
Zero-energy campus buildings	10 - 180	5	5000 - 15000	200
Zero-energy office buildings	10 - 130	3	5000 - 30000	500
Zero-energy residential buildings	10 - 90	2	5000 - 30000	500

Three optimization criteria are considered in the multi-objective optimization including the time-of-use grid penalty cost (PC_{TOU}) as per Eq. (5), self-consumption ratio (SCR) as per Eq. (6) and load cover ratio (LCR) as per Eq. (7).

The SCR of hybrid renewable energy and storage systems is formulated as Eq. (6) to evaluate the utilization efficiency of renewable power supply:

$$SCR = \frac{on\text{-}site\ RE\ consumption}{total\ RE\ generation} = \frac{E_{RE\ to\ load} + E_{RE\ to\ battery} + E_{RE\ to\ electrolyzer}}{E_{RE}} \quad (6)$$

where $E_{RE\ to\ load}$ is the produced renewable energy from PV and wind sources to meet the electrical load of buildings, kWh. $E_{RE\ to\ battery}$ is the produced renewable energy supplied to charge batteries, kWh. $E_{RE\ to\ electrolyzer}$ is the produced renewable energy supplied to drive electrolyzers of hydrogen systems to generate hydrogen, kWh. E_{RE} is the total renewable energy generation, kWh.

The *LCR* is developed to estimate the on-site coverage of the electrical load by hybrid renewable energy and storage systems as per Eq. (7):

$$LCR = \frac{on\text{-}site\ supply}{total\ electrical\ load} = \frac{E_{RE\ to\ load} + E_{battery\ to\ load} + E_{FCs\ to\ load}}{E_{load}} \quad (7)$$

where $E_{battery\ to\ load}$ is the energy discharged from battery units to meet the load, kWh. $E_{FCs\ to\ load}$ is the energy from fuel cells of hydrogen systems to the load, kWh. E_{load} is the total electrical load including building demand and energy required for hydrogen compression, kWh.

(2) Evaluation of zero-energy buildings and community

To further evaluate the economic performance of zero-energy buildings and the community compared with baseline scenarios without renewable energy, the lifetime net present value (*NPV*) including the investment cost of renewable energy systems, grid feed-in tariff (FiT) and time-of-use electricity bill is formulated as Eq. (8).

$$NPV = PRV_{investment} - PRV_{FiT} + PRV_{bill} \quad (8)$$

where $PRV_{investment}$ is the present value of investment of hybrid systems, US$. PRV_{FiT} is the present value of feed-in tariff, US$. PRV_{bill} is the present value of electricity bill for grid import energy, US$.

The present value of investment of hybrid systems includes the present value of initial cost (PRV_{ini}), present value of operation and maintenance cost ($PRV_{O\&M}$), present value of replacement cost (PRV_{rep}) and present value of residual cost (PRV_{res}) as per Eq. (9). The system components cover PV panels, wind turbines, inverters, battery units, electrolyzers, compressors, hydrogen storage tanks and HVs.

$$\begin{aligned} PRV_{investment} &= PRV_{ini} + PRV_{O\&M} + PRV_{rep} - PRV_{res} \\ &= C_{ini} + \sum_{n=1}^{n=N} \frac{f_{mai} \cdot C_{ini}}{(1+i)^n} + \sum_{j=1}^{j=J} C_{ini} \left(\frac{1-d}{1+i}\right)^{j \cdot l} - C_{ini} \frac{l_{res}}{l} \cdot \frac{(1-d)^N}{(1+i)^N} \end{aligned} \quad (9)$$

where C_{ini} is the initial cost of hybrid systems, US$. i is the annual real discounted rate (0.058/year [48]). n is the specific year and N is the system lifetime (20 years). f_{mai} is the proportion of the operation and maintenance cost to the initial cost including insurance [49]. j is the specific replacement number and J is the total replacement number. d is the annual cost degradation rate. l is the lifetime and l_{res} is the residual lifetime. The economic parameters of the hybrid renewable energy and storage systems are shown in Table 2.

Table 2 Economic parameters of the hybrid renewable energy and storage systems

Components	Initial cost	O&M ratio (of initial cost)	Lifetime, year	Annual price degradation rate
PV panel [50]	3500 US$/kW	2%	20	--
Wind turbine [50]	4000 US$/kW	1%	20	--
Battery [50]	1000 US$/kWh	1%	5 [51]	5%/year [52]
Inverter/converter [50]	700 US$/kW	1%	10	10.15%/year [53]
Electrolyzer	1400 US$/kW [10]	2% [54]	20 [55]	--
Compressor	15000 US$/Set [56]	2% [57]	20 [58]	--
H_2 storage tank [54]	50 US$/N m^3	0.50%	25	4.2%/year [59]
Hydrogen vehicle [60]	58500 US$/HV	2%	8	4.3%/year [61]

It is assumed all renewable generation can get the FiT subsidy at the local FiT rate as per Eq. (10) and the on-site used renewable electricity is charged at the time-of-use tariff rate counted in the electricity bill item according to the local FiT scheme [62].

$$PRV_{FiT} = \sum_{n=1}^{n=N} \frac{\left(E_{PV}\cdot(1-\delta_{PV})^{n-1} + E_{WT}\cdot(1-\delta_{WT})^{n-1}\right)\cdot c_{fit}}{(1+i)^n} \quad (10)$$

where E_{PV} is the annual energy production of the PV system, kWh. δ_{PV} is the degradation rate of the PV system (1%/year [63]). E_{WT} is the annual energy production of the wind system, kWh. δ_{WT} is the degradation rate of the wind system (1.5%/year [64]). c_{fit} is the local feed-in tariff rate (3 HK$/kWh [62]).

The electricity bill for grid imported energy includes the demand charge, energy charge, fuel cost adjustment, rent and rates special rebate according to the local time-of-use tariff for buildings with large power demand [43] as per Eq. (11).

$$PRV_{bill} = \sum_{n=1}^{n=N} \frac{(Bill_{demand} + Bill_{energy} + Bill_{fuel} - Bill_{rebate}) \cdot \varepsilon}{(1+i)^n} \tag{11}$$

where $Bill_{demand}$ is the annual demand charge of time-of-use electricity tariff, HK$. $Bill_{energy}$ is the annual energy charge, HK$. $Bill_{fuel}$ is the annual fuel cost adjustment, HK$. $Bill_{rebate}$ is the annual rent and rates special rebate, HK$. ε is the exchange rate of HK$ and US$. The detailed formulation of these electricity bill items is shown as Eqs. (12-15).

$$\begin{aligned} Bill_{demand} = {} & \text{MIN}(5000 \cdot 12, P_{max\_on} \cdot 12) \cdot 120.3 + \text{MAX}(0, P_{max\_on} \cdot 12 - 5000 \cdot 12) \cdot 115.3 \\ & + \text{MAX}(0, P_{max\_off} \cdot 12 - P_{max\_on} \cdot 12) \cdot 33.9 \end{aligned} \tag{12}$$

$$\begin{aligned} Bill_{energy} = {} & \text{MIN}\left(E_{sum\_on}, 200 \cdot P_{max\_on} \cdot 12\right) \cdot 0.567 + \text{MAX}\left(0, E_{sum\_on} - 200 \cdot P_{max\_on} \cdot 12\right) \cdot \\ & 0.547 + E_{sum\_off} \cdot 0.469 \end{aligned} \tag{13}$$

$$Bill_{fuel} = (E_{sum\_on} + E_{sum\_off}) \cdot 0.298 \tag{14}$$

$$Bill_{rebate} = (E_{sum\_on} + E_{sum\_off}) \cdot 0.012 \tag{15}$$

where P_{max_on} is the annual maximum imported power during on-peak time, kW. P_{max_off} is the annual maximum imported power during off-peak time, kW. E_{sum_on} is the total annual imported energy during on-peak time, kWh. E_{sum_off} is the total annual imported energy during off-peak time, kWh.

The annual equivalent carbon emissions (CE_a) is also calculated to assess the decarbonisation potential of zero-energy scenarios compared with baseline scenarios without renewable energy applications as shown in Eq. (16) [65].

$$CE_a = (E_{grid\ import} - E_{grid\ export}) \cdot CEF_{eq} \tag{16}$$

where $E_{grid\ import}$ is the total annual electricity imported from the utility grid, kWh. $E_{grid\ export}$ is the total annual electricity exported to the utility grid, kWh. CEF_{eq} is the equivalent CO_2 emission factor (0.572 $kgCO_2/kWh$ [65]), and the equivalent carbon emission cost subject to the local social cost of carbon (0.024 US$/$kgCO_2$ [66]) is also evaluated.

3. Results and discussion

3.1. Design optimization results of zero-energy buildings and community

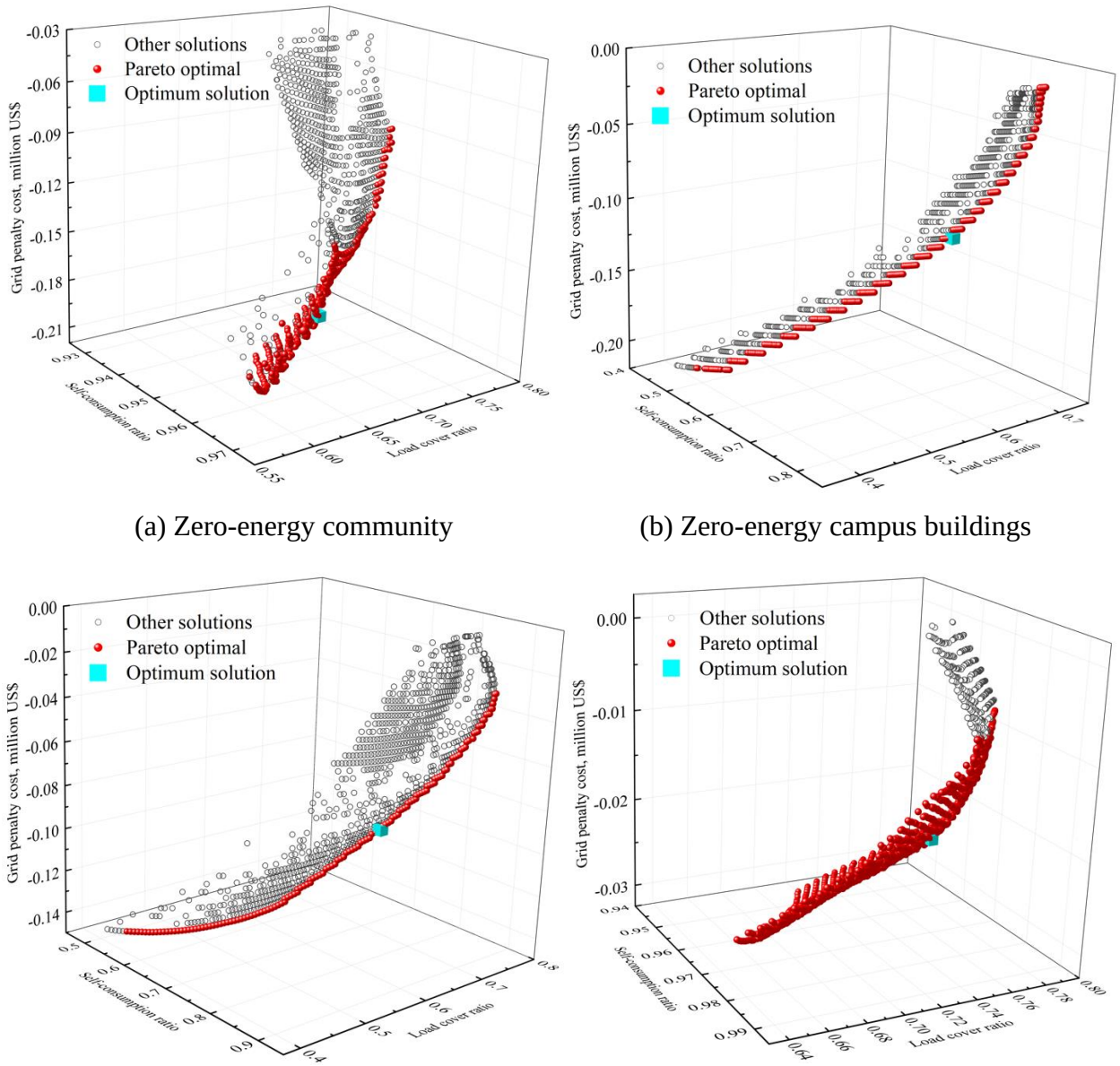

(a) Zero-energy community (b) Zero-energy campus buildings

(c) Zero-energy office buildings (d) Zero-energy residential buildings

Fig. 7 Pareto optimal and final optimum solution of four zero-energy scenarios

Multi-objective optimizations are conducted to size the hybrid systems for four zero-energy building scenarios. Fig. 7 shows the distribution of Pareto optimal solutions among all searched solutions for optimizing *SCR*, *LCR* and PC_{TOU}. It indicates clear trade-off conflicts among the focused optimization criteria in all four zero-energy scenarios. A final optimum solution is selected

from the Pareto optimal set in each scenario as highlighted in cyan cube according to the minimum distance to the utopia point method [47]. The sizing results of hybrid renewable energy and storage systems for four zero-energy building scenarios are shown in Table 3.

Table 3 Sizing results of renewable energy and storage systems for four zero-energy scenarios

Sizing results	PV /kW	Wind turbine /kW	Battery /kWh
Zero-energy community	75095	8000	33000
Zero-energy campus buildings	21604	8500	15000
Zero-energy office buildings	23200	3400	30000
Zero-energy residential buildings	11571	4200	17500

3.2. System supply performance of zero-energy buildings and community

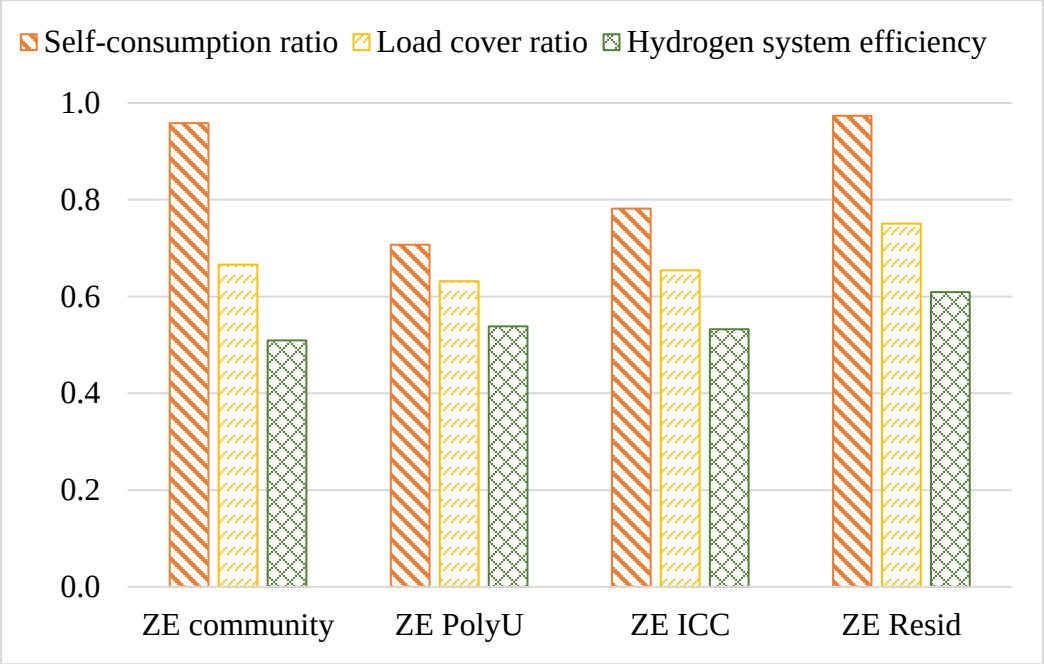

Fig. 8 Supply performance of renewable energy systems of zero-energy scenarios with battery storage

The system supply performance of hybrid systems of four zero-energy building scenarios with battery and hydrogen vehicle storage is shown in Fig. 8. It is found that the maximum *SCR* and *LCR* of 97.33% and 75.06% are achieved in the zero-energy Resid group with the lowest

building load and best charging availability of HVs. While the minimum *SCR* and *LCR* of 70.70% and 63.14% is achieved in the zero-energy PolyU group with the highest building load and minimum HV number. The *SCR* and *LCR* of the zero-energy community integrating three building groups outperform the PolyU group and ICC group but are slightly lower than the Resid group. The zero-energy Resid group has the highest *HSE* of about 60.92% with a high HV number and more parking time available for energy exchange with the supply and buildings. And the *HSE* can be reduced to about 42.66% when the generated heat from electrolyzers, compressors and PEMFCs is not recovered for domestic hot water production. The *HSE* of the other three zero-energy building scenarios is comparatively lower between 50.96% - 53.83% with less HVs and lower charging availability.

Table 4 System supply performance of zero-energy scenarios with and without battery storage

System supply performance	Self-consumption ratio (*SCR*)	Load cover ratio (*LCR*)	Hydrogen system efficiency (*HSE*)
ZE community	95.86%	66.62%	50.96%
ZE PolyU	70.70%	63.14%	53.83%
ZE ICC	78.19%	65.39%	53.22%
ZE Resid	97.33%	75.06%	60.92%
ZE community - no battery	95.55% (-0.32%)	62.16% (-6.70%)	50.02% (-1.84%)
ZE PolyU - no battery	61.68% (-12.77%)	55.03% (-12.84%)	56.51% (4.98%)
ZE ICC - no battery	56.10% (-28.25%)	46.45% (-28.96%)	53.78% (1.05%)
ZE Resid - no battery	98.48% (1.19%)	68.94% (-8.15%)	64.77% (6.32%)

Table 4 compares the system supply performance of hybrid systems of four zero-energy building scenarios with and without battery storage indicating their relative difference. It is shown that the *SCR* of the PolyU group and ICC group is reduced by 12.77% and 28.25% respectively when battery storage is removed from zero-energy building scenarios, because less renewable energy is consumed by on-site demand and storage especially during periods when HVs are on cruise. However, the *SCR* in the Resid group is slightly improved by 1.19% without battery storage

because of higher renewable energy consumption by the large HV group with accessible charging periods. The *LCR* of all four scenarios is reduced when the battery storage is excluded from zero-energy buildings. Especially, up to 28.96% decline is observed in the ICC group as less on-site renewable energy is available to meet the building electrical load without batteries. The storage efficiency of hydrogen systems excluding the cruise consumption under all scenarios is slightly improved under the system without batteries, because the battery storage is prioritized over hydrogen storage in original zero-energy scenarios with battery storage, so that more energy storage is available for hydrogen storage when the battery is absent. While the overall efficiency of hydrogen systems considering the cruise consumption of the zero-energy community scenario without battery storage is reduced by 1.84% compared with the scenario with battery storage because the road consumption is relatively large and independent of the battery storage. It is also indicated that the *SCR, LCR* and *HSE* are all improved for the zero-energy community scenario when battery storage is installed.

3.3. Economic performance and decarbonisation potential of zero-energy buildings and community

The economic performance and decarbonisation potential of zero-energy buildings and the community with hybrid PV-wind-battery-hydrogen systems are analyzed and compared with baseline scenarios without renewable energy. It is assumed that HV groups are included in baseline scenarios meeting the daily commuting demand of building occupants but refilled in external hydrogen stations at a cost of 16.51 US$/kg [67]. And zero-energy scenarios with hybrid PV-wind-hydrogen systems but without battery storage is also developed for comparison to study the impact of battery storage. The grid penalty cost, lifetime *NPV* and annual carbon emissions of baseline scenarios without renewable energy, zero-energy scenarios with battery storage and zero-energy scenarios without battery storage are compared.

(1) Grid penalty cost

The grid penalized energy during on-peak and off-peak periods of the buildings and the community under three systems is compared in Fig. 9. The positive penalized energy would result in a grid cost punishment and the negative penalized energy would result in a grid reward to occupants as explained in Section 2.3. It is indicated that the grid penalized energy during both off-peak and on-peak time of the community, PolyU and ICC buildings under the baseline scenario

are positive with a fine, while it is negative with a bonus during on-peak time for the Resid buildings. Because the grid imported energy during on-peak time for the Resid buildings is relatively small and less than its grid import estimation. Obvious economic reward can be achieved for on-peak grid import and off-peak grid export for all buildings and the community integrating renewable energy systems with negative penalized energy.

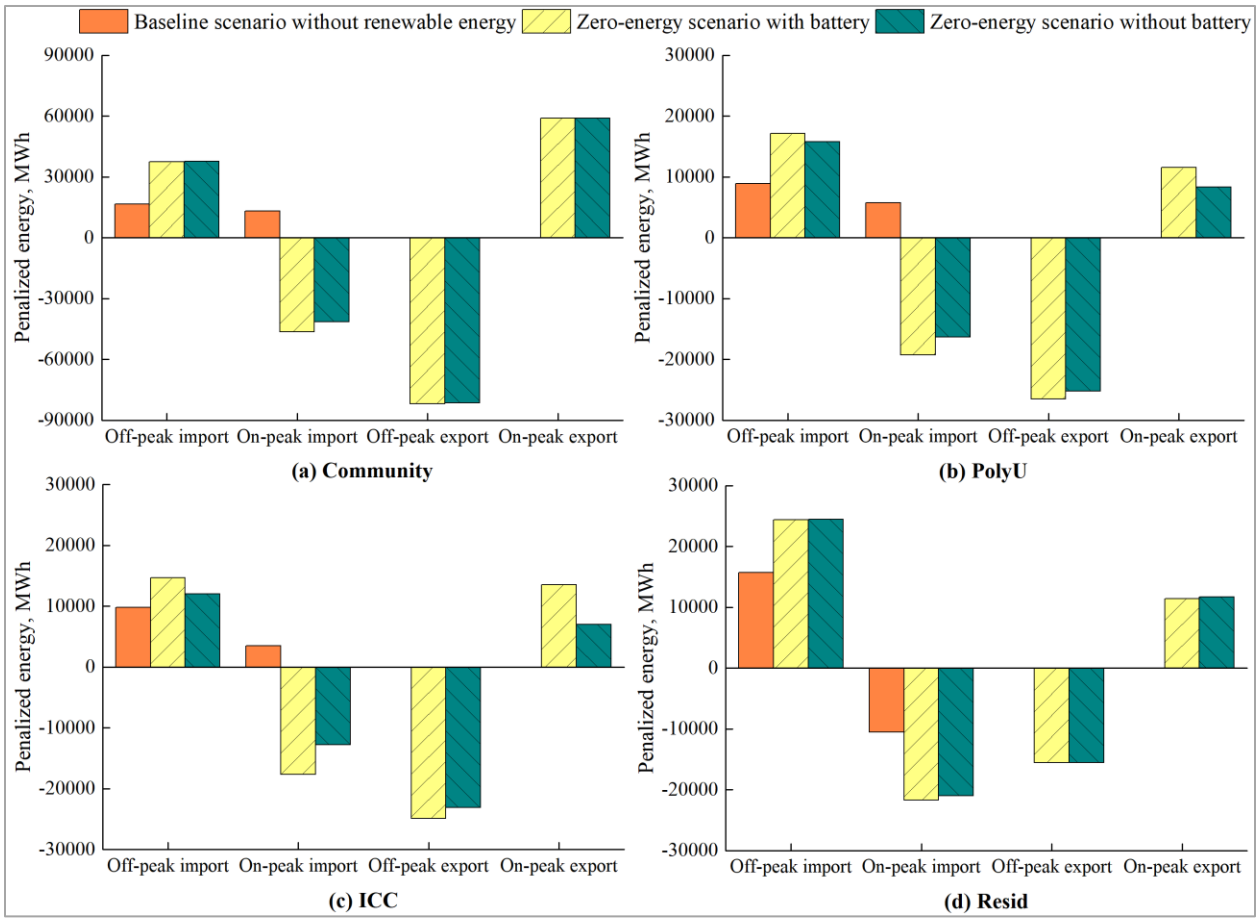

Fig. 9 Grid penalized energy of buildings and community under three systems

The annual net grid import energy and grid penalty cost of three buildings and community under three different scenarios are compared in Fig. 10. It is indicated that the annual net grid import energy of the Resid group is the minimum (27206.11 MWh) among four baseline scenarios as per Fig. 10(a) because the annual electrical load of residential buildings is the minimum. The net grid import energy is significantly reduced in zero-energy scenarios with battery storage by 71.23% - 90.93% compared with baseline scenarios without renewable energy. And a net grid import reduction of up to 91.36% is observed in the zero-energy PolyU group without battery

storage (4554.23 MWh) compared with the corresponding baseline scenario as more renewable generation is fed into the utility grid.

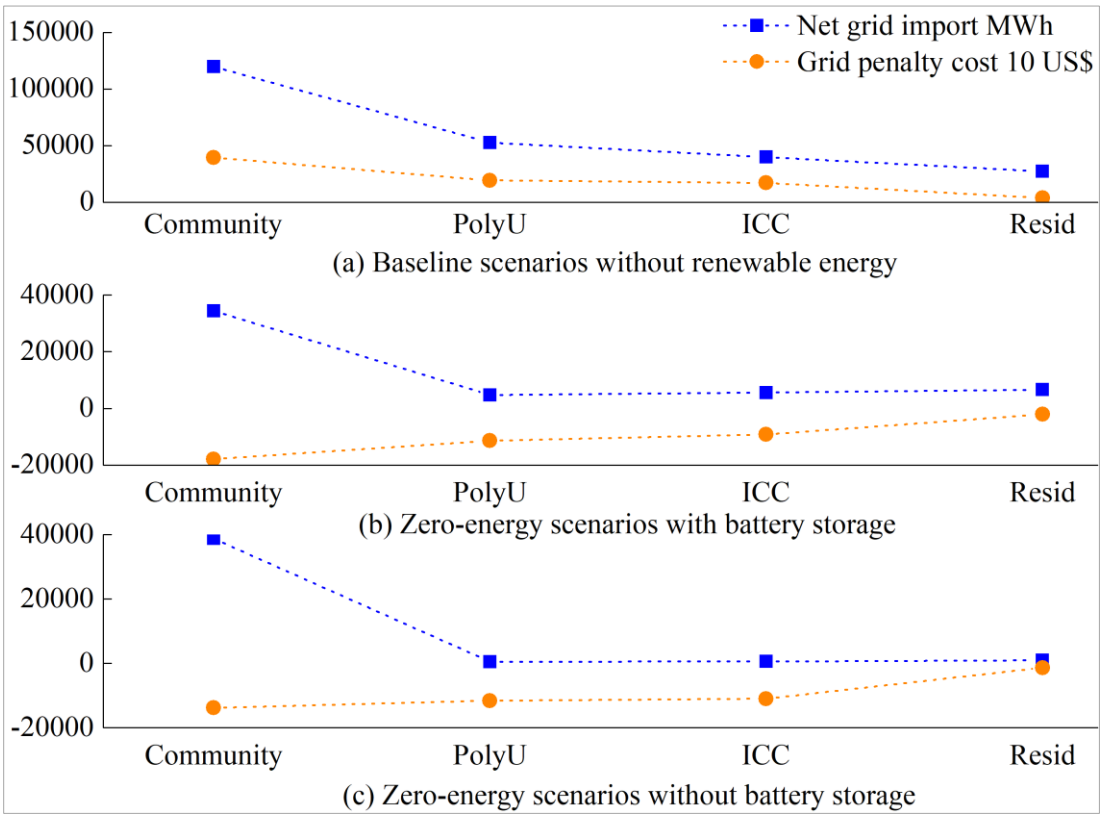

Fig. 10 Grid integration performance of buildings and community under three systems

The grid integration improvement of zero-energy buildings and the community is compared in Table 5 indicating the relative difference on top of baseline scenarios. The grid penalty cost of four baseline scenarios ranges from US$ 37916.41 to US$ 393649.96 with the minimum achieved in the Resid group for the less building load and energy consumption during on-peak hours. On the contrary, the grid penalty cost of all zero-energy scenarios is negative as a bonus contributing to relieving the utility grid with higher operational flexibility and economy performance. Specifically, a reduction of up to 145.36% - 158.92% on the grid penalty cost is achieved in zero-energy scenarios with battery storage compared with baseline scenarios. And the maximum reduction of 164.41% on the grid penalty cost is observed in the zero-energy ICC group without battery storage. The PolyU group gets the highest grid bonus compared with the ICC and Resid groups under zero-energy scenarios indicating more grid export during on-peak time and less grid import during off-peak time. The community integrating three building groups with different

operational schedules gets more grid reward with higher grid flexibility than three individual building groups in zero-energy scenarios. The grid penalty cost of the community is about US$ -178559.85 in zero-energy scenarios with battery storage, and it is 29.40% lower than that of zero-energy scenario without battery storage. So the battery storage can significantly contribute to the grid relief of the community.

Table 5 Grid integration improvement of zero-energy buildings and the community

Grid integration	Net grid import MWh	Grid penalty cost US$
Baseline scenarios without renewable energy		
Community	119714.05	393649.96
PolyU	52740.46	192643.05
ICC	39767.47	170569.33
Resid	27206.11	37916.41
Zero-energy scenarios with battery storage		
Community	34445.58 (-71.23%)	-178559.85 (-145.36%)
PolyU	4786.04 (-90.93%)	-113500.47 (-158.92%)
ICC	5565.94 (-86.00%)	-92066.53 (-153.98%)
Resid	6645.33 (-75.57%)	-20679.02 (-154.54%)
Zero-energy scenarios without battery storage		
Community	38821.67 (-67.57%)	-137991.69 (-135.05%)
PolyU	4554.23 (-91.36%)	-115692.02 (-160.06%)
ICC	4777.33 (-87.99%)	-109863.97 (-164.41%)
Resid	7590.23 (-72.10%)	-13336.13 (-135.17%)

(2) Lifetime net present value

The net present value (*NPV*) of the PolyU, ICC and Resid building groups and the community during a 20-year lifetime under three different scenarios is analyzed as per Fig.11. The lifetime *NPV* of baseline scenarios without renewable energy mainly covers the electricity bill of the building load and investment of HVs including the initial cost, O&M cost, replacement cost and residual cost. The cost of hydrogen refill by external hydrogen stations is included in the O&M cost. And the lifetime *NPV* of zero-energy scenarios includes the investment of renewable energy components, electricity bill and FiT subsidy. The FiT subsidy is obtained in zero-energy scenarios

at an FiT rate of 3 HK$ for all units of electricity generated by the renewable energy system, and the on-site consumed renewable generation is charged at the time-of-use electricity rate [62].

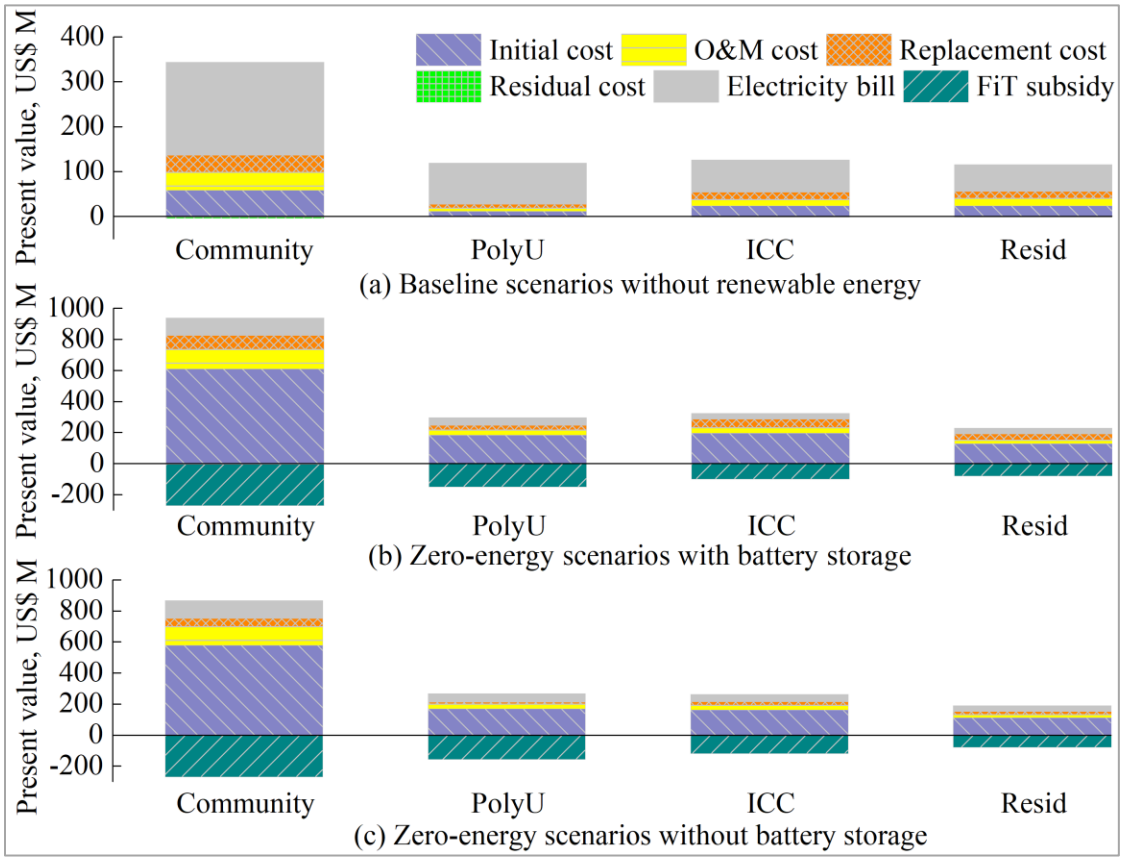

Fig. 11 Lifetime net present value of buildings and community under three systems

It is shown that the electricity bill accounts for the majority of the lifetime *NPV* in baseline scenarios as per Fig. 11(a) at about 52.26% - 77.85% for four building scenarios as the electrical load is totally met by the utility grid. The lifetime electricity bill of the community at about US$ 207.47M is lower than the sum of electricity bills of three building groups by US$ 15.90M. The initial cost of the renewable energy system contributes to the main part of lifetime cash outflows (i.e. investment and electricity bill) under all four zero-energy scenarios with battery storage at 56.79% - 65.41% and four zero-energy scenarios without batteries at 59.25% - 67.04%. A favorable amount of FiT subsidy can be achieved at US$ 77.37M - 265.62M for zero-energy scenarios with battery storage and US$ 76.47M - 265.79M for zero-energy scenarios without battery storage. The maximum FiT subsidy is obtained in the community scenario with the maximum renewable energy generation.

Table 6 Economic analysis of buildings and community under three systems

Present value million US$	Initial cost	O&M cost	Replacement cost	Residual cost	Electricity bill	FiT subsidy	Lifetime net present value
Baseline scenarios without renewable energy							
Community	58.50	40.25	37.97	-3.93	207.47	0.00	340.25
PolyU	11.70	7.66	7.59	-0.79	91.97	0.00	118.13
ICC	23.40	15.31	15.19	-1.57	71.97	0.00	124.30
Resid	23.40	17.28	15.19	-1.57	59.43	0.00	113.73
Zero-energy scenarios with battery storage							
Community	610.29	127.95	86.38	-3.93	112.38	-265.62	667.45 (96.17%)
PolyU	183.44	34.60	28.55	-0.79	48.89	-150.11	144.58 (22.39%)
ICC	195.59	38.35	52.52	-1.57	36.94	-98.10	223.72 (79.99%)
Resid	128.74	24.73	37.00	-1.57	37.79	-77.37	149.32 (31.30%)
Zero-energy scenarios without battery storage							
Community	577.63	124.18	49.31	-3.93	114.45	-265.79	595.86 (75.12%)
PolyU	168.44	32.86	11.70	-0.79	54.26	-155.96	110.51 (-6.45%)
ICC	161.45	33.89	18.82	-1.57	47.02	-116.21	143.40 (15.37%)
Resid	111.41	22.73	17.34	-1.57	38.12	-76.47	111.57 (-1.90%)

Table 6 lists detailed items of lifetime *NPV* of three building groups and their community under three systems. It is indicated that the lifetime *NPV* of four baseline scenarios varies between US$ 113.73M - 340.25M including the HV investment and grid electricity bill. The lifetime *NPV* of four zero-energy scenarios with battery storage is increased compared with baseline scenarios due to large investment of renewable energy systems. The zero-energy community powered by the hybrid PV-wind-battery-hydrogen system shows a 96.17% *NPV* increment and a relatively low increment of 22.39% is observed in the zero-energy PolyU group with batteries. The lifetime *NPV* of the Reside group is about US$ 149.32M, which is slightly higher than the PolyU group with

more FiT subsidy. It is also highlighted that the lifetime *NPV* of zero-energy scenarios without batteries is obviously lower than zero-energy scenarios with batteries due to the high initial cost and regular replacement of batteries. The lifetime *NPV* is lowered by about 6.45% of US$ 7.62M for the PolyU group without batteries and 1.9% of US$ 2.16M for the Resid group without batteries compared with baseline scenarios. While the *NPV* of the community and ICC group without batteries is increased by 75.12% and 15.37% respectively on top of baseline scenarios. As a result, economic benefits can be obtained by applying hybrid PV-wind-hydrogen systems in the PolyU and Resid groups compared with corresponding baseline scenarios.

(3) Carbon emissions and equivalent carbon emission cost

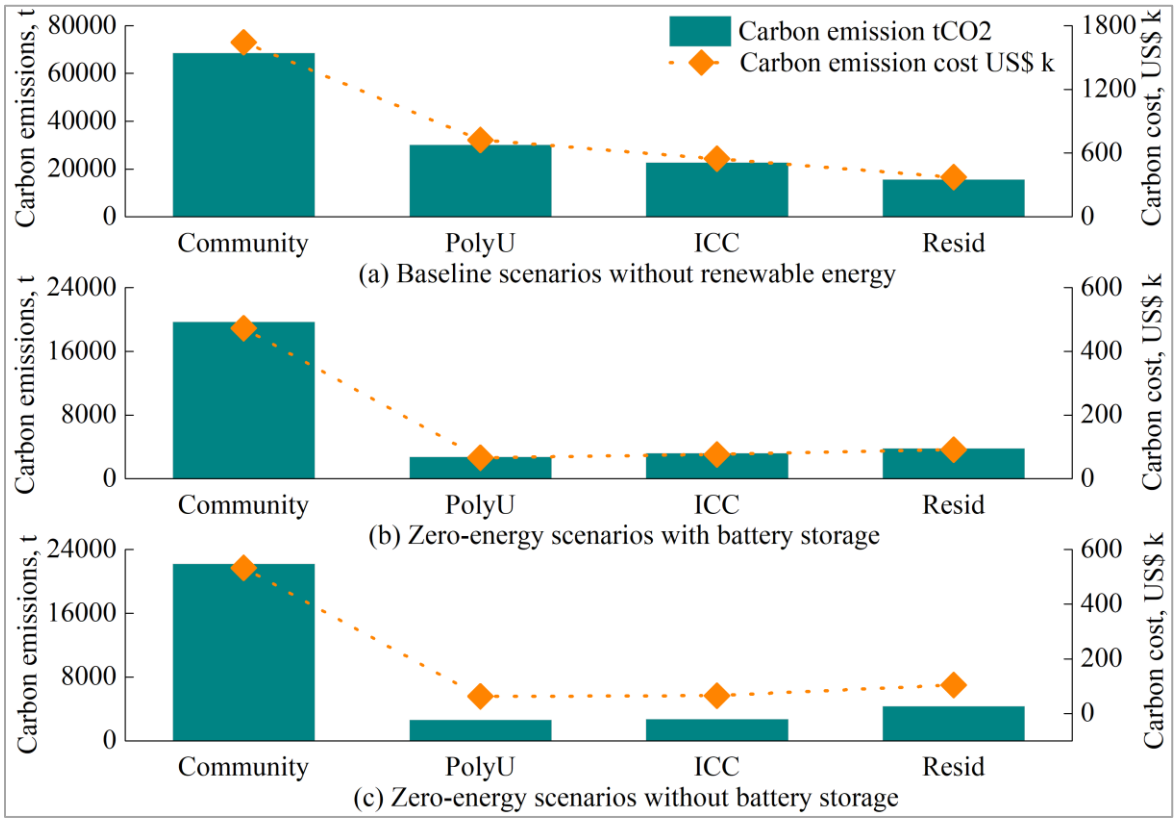

Fig. 12 Carbon emissions and equivalent carbon emission cost of buildings and community under three systems

The annual carbon emissions and equivalent carbon emission cost of three building groups and their community are compared for the three scenarios as per Fig. 12. It is shown that the annual carbon emissions and carbon emission cost of the baseline Resid group (15561.90 tCO_2 and US$ 373.49k) are less than those of the baseline PolyU group and Resid group due to lower annual

electrical load of the residential buildings. While the carbon emissions and carbon emission cost of the PolyU group are the minimum in zero-energy building scenarios with the largest amount of renewable energy generation and maximum grid export. The annual carbon emissions of the community integrating three building groups is considerably higher than the sum of carbon emissions of three buildings in zero-energy scenarios. Because more renewable generation in the community is consumed on-site with a small amount fed into the utility grid while a relatively large amount imported from the grid although lower than the grid imported sum of three buildings.

Table 7 Decarbonisation potential of zero-energy buildings and the community

Carbon emission analysis	Carbon emissions tCO_2	Equivalent carbon emission cost US$ k
Baseline scenarios without renewable energy		
Community	68476.43	1643.43
PolyU	30167.55	724.02
ICC	22746.99	545.93
Resid	15561.90	373.49
Zero-energy scenarios with battery storage		
Community	19702.87 (-71.23%)	472.87 (US$ -1170.57k)
PolyU	2737.61 (-90.93%)	65.70 (US$ -658.32k)
ICC	3183.72 (-86.00%)	76.41 (US$ -469.52k)
Resid	3801.13 (-75.57%)	91.23 (US$ -282.26k)
Zero-energy scenarios without battery storage		
Community	22206.00 (-67.57%)	532.94 (US$ -1110.49k)
PolyU	2605.02 (-91.36%)	65.52 (US$ -661.50k)
ICC	2732.63 (-87.99%)	65.58 (US$ -480.34k)
Resid	4341.61 (-72.10%)	104.20 (US$ -269.29k)

The decarbonisation potential of zero-energy buildings and community is compared with baseline scenarios as per Table 7 with an indication of the relative difference. It is indicated that obvious reductions in carbon emissions and carbon emission cost are achieved for zero-energy scenarios compared with baseline scenarios entirely relying on the utility grid and external hydrogen refill. Specifically, the carbon emissions decline by 71.23% - 90.93% in four zero-energy scenarios with battery storage with a carbon emission cost saving of US$ 282.26k - 1170.57k. The carbon emission reduction potential of the community in zero-energy scenarios without battery storage is 67.57% based on baseline scenarios. It is slightly lower than that in zero-energy scenarios with battery storage due to a higher grid import when the battery storage is absent from the community. The maximum carbon emission saving potential is achieved in the zero-energy PolyU group without battery storage with a carbon emission decline of up to 91.36% for about 27562.53 tCO_2 compared with the baseline scenario. And the maximum carbon emission cost saving potential is obtained in the zero-energy community with battery storage at about US$ 1170.57k compared with the baseline scenario relying on the utility grid and external hydrogen refill.

3.4. Sensitivity analysis on time-of-use grid penalty cost model

The grid import estimation is defined as the ratio of the peak building electrical load and the grid export estimation is defined as the ratio of the rated renewable energy capacity as explained in the time-of-use grid penalty cost model in Section 2.3. A sensitivity analysis is conducted to investigate the impact of these two ratios on the grid penalty cost for the zero-energy community with battery storage. It is indicated from Fig. 13 (a) that the penalty cost of grid import power during off-peak time increases with the import estimation ratio as a low import estimation is preferred by the utility grid to encourage more excess import in off-peak time. While the penalty cost of grid import power during on-peak time shows a negative correlation with the import estimation ratio because a high import estimation is preferred by the utility grid to reduce unplanned grid import in on-peak time. The penalty cost of grid export is however not affected by the import estimation ratio. Fig. 13(b) shows that the penalty cost of grid export in off-peak time declines with the export estimation ratio while the grid export penalty cost in on-peak time shows an opposite correlation as excess grid export is discouraged during off-peak time but welcomed during on-peak time. The total time-of-use grid penalty cost is US$ -178.56k under the assumed condition with an import estimation ratio of 50% and export estimation ratio of 20%. Large

amounts of bonus are achieved for both grid export in off-peak time ($PC_{export\_offpeak}$) at US$ -499.18k as per Fig. 13(a) and grid import in on-peak time (PC_{import_onpeak}) at US$ -338.88k as per Fig. 13(b). While a fine is imposed for both grid export in on-peak time (PC_{export_onpeak}) at US$ 430.96k and grid import in off-peak time ($PC_{import\_offpeak}$) at about US$ 228.54k. Appropriate grid import and export estimation ratios should be set in zero-energy building applications based on the grid power availability considering the peak electrical load and rated renewable energy capacity.

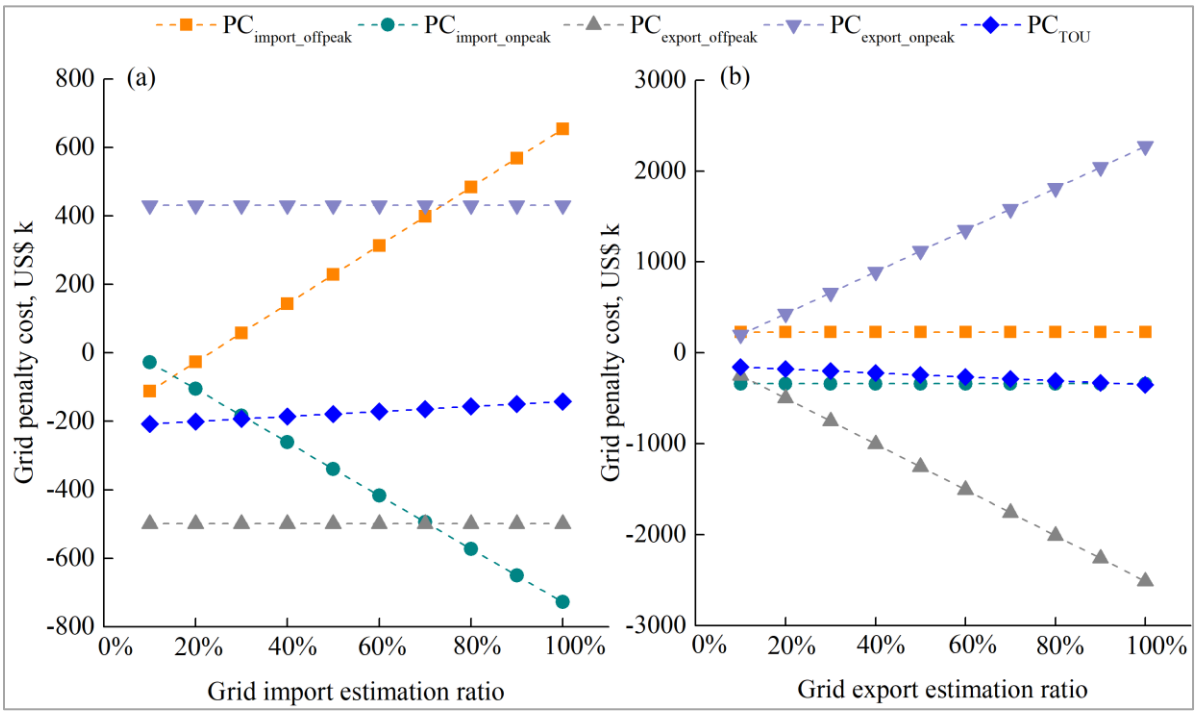

Fig. 13 Impact of grid import estimation ratio and grid export estimation ratio on grid penalty cost of zero-energy community with battery storage

The impact of the penalty factor ratio of the grid penalty cost model is illustrated in Fig. 14. It is indicated that absolute values of penalty cost of grid import and grid export in both off-peak and on-peak time increase with the penalty factor. The penalty cost of grid import during off-peak time and grid export during on-peak time is positive with a fine to the community microgrid to charge unreached grid import in off-peak time and unmet grid export in on-peak time. While the penalty cost of grid import in on-peak time and grid export in off-peak time is negative with a bonus to the community microgrid to reward unused grid import in on-peak time and unfed grid export in off-peak time. The total time-of-use penalty cost with the penalty factor ratio of 10% is

about US$ -178.56k, which can compensate for about 1.01% of the annual electricity bill of the zero-energy community. And the maximum time-of-use penalty cost with the penalty factor ratio of 100% is about US$ -1785.60k accounting for about 10.08% of the annual electricity bill.

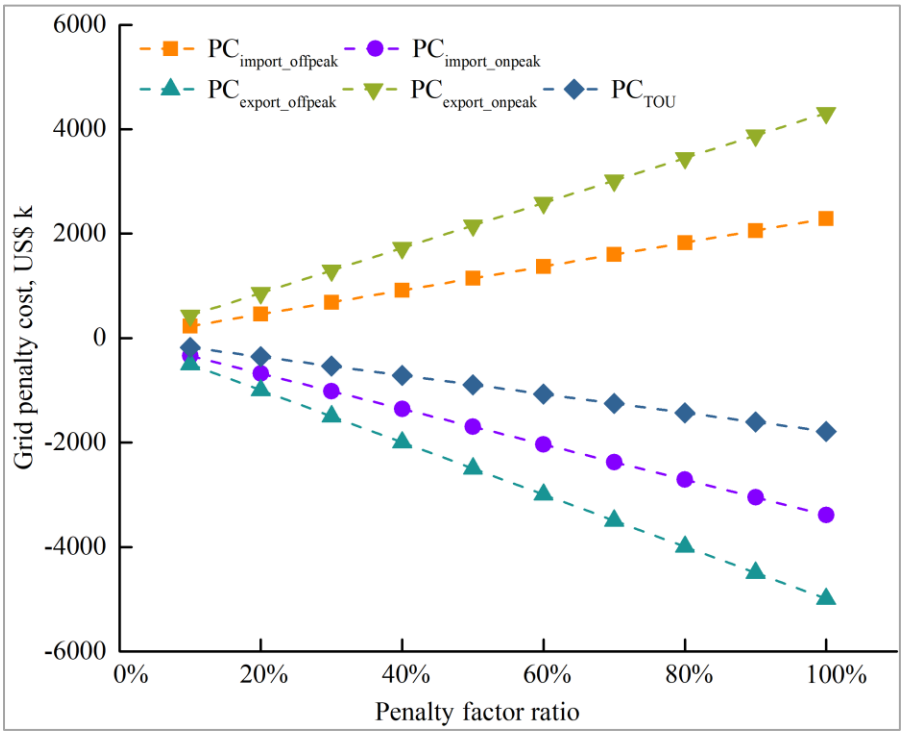

Fig. 14 Impact of penalty factor ratio on grid penalty cost of the zero-energy community with battery storage

3.5. Research significance, limitations and future work

This study develops hybrid renewable energy systems integrated with stationary battery and mobile hydrogen vehicle storage for zero-energy buildings and their community in urban areas. A time-of-use grid penalty cost model is proposed to improve the power flexibility and economy between the zero-energy microgrid system and utility grid. Multi-objective optimizations are conducted to size hybrid renewable energy and storage systems for four zero-energy scenarios. The techno-economic-environmental feasibilities of zero-energy scenarios with and without stationary battery storage are identified in comparison with baseline scenarios without renewable energy. The research results can guide relative stakeholders to develop renewable energy applications for zero-energy buildings and communities in urban areas. And the proposed time-of-use grid penalty cost model provides significant references to achieve power grid resilience and

economy for grid-connected large-scale renewable energy system deployment in urban communities. However, this research has not considered the degradation in the operation and management of the stationary battery storage. Further research will be conducted on dynamic battery degradation integrated with renewable energy systems for power supply to zero-energy communities. And the zero-energy community integrating renewable energy systems with Li-ion battery vehicles will also be studied considering the battery management and optimization.

4. Conclusions

This study develops shared hybrid renewable energy and storage microgrid systems for a zero-energy community consisting of campus, office and residential buildings based on a combination of on-site collected and simulated building energy data. Three mobile hydrogen vehicle groups following different cruise schedules are integrated as transportation tools and shared storage units together with stationary batteries. Multi-objective optimizations are conducted to size three zero-energy buildings and the integrated zero-energy community by coupling jEplus+EA with TRNSYS. Four zero-energy scenarios without stationary battery storage and four baseline scenarios without renewable energy are also developed for the techno-economic-environmental performance comparison. Important findings are concluded as below:

(1) The zero-energy residential building group achieves the maximum renewable energy self-consumption ratio, load cover ratio and hydrogen system efficiency of about 97.33%, 75.06% and 60.92% in four zero-energy scenarios with battery storage. Battery storage improves the self-consumption ratio, load cover ratio and hydrogen system efficiency performance of the zero-energy community and enhances the load cover ratio of all four zero-energy scenarios by up to 28.96% in the office building group.

(2) A time-of-use grid penalty cost model evaluating grid import and grid export during on-peak and off-peak periods is developed to achieve the flexibility and economy between the renewable energy microgrid and utility grid. It is suggested that appropriate grid import and export estimation ratios should be set in zero-energy building and community applications based on the grid power availability considering the peak electrical load and rated renewable energy capacity.

(3) The net grid import energy is reduced by 71.23% - 90.93% in four zero-energy scenarios with battery storage and by 72.10% - 91.36% in four zero-energy scenarios without battery storage compared with baseline scenarios without renewable energy. The grid penalty cost reductions of

145.36% - 158.92% and 135.05% - 164.41% are achieved in zero-energy scenarios with and without battery storage compared with baseline scenarios. The zero-energy community has higher grid flexibility with lower grid penalty cost than three individual building groups. Battery storage contributes to the grid relief of the zero-energy community with a 29.40% penalty cost reduction.

(4) The lifetime net present value of four zero-energy scenarios with battery storage is increased by 22.39% - 96.17% compared with baseline scenarios. The lifetime net present value of the community and office building group without battery storage is increased by 75.12% and 15.37% respectively on top of baseline scenarios. While the net present value is reduced by about 6.45% of US$ 7.62M and 1.90% of US$ 2.16M for the campus and residential building group without battery storage compared with baseline scenarios. Therefore, economic benefits can be obtained by applying hybrid renewable energy and hydrogen vehicle storage systems to the campus and residential building groups.

(5) Substantial environmental benefits can be achieved in all zero-energy scenarios with significant reductions in carbon emissions and costs compared with baseline scenarios. The carbon emissions decline by 71.23% - 90.93% in four zero-energy scenarios with battery storage achieving a carbon emission cost saving of US$ 282.26k - 1170.57k. And about 67.57% - 91.36% of the carbon emission reduction for a cost of US$ 269.29k - 1110.49k can be achieved in four zero-energy scenarios without battery storage.

(6) The comprehensive feasibility study of zero-energy buildings and their community is presented considering the system supply performance, lifetime cost and decarbonisation potential. The detailed comparison results based on zero-energy scenarios without battery storage and baseline scenarios without renewable energy offer clear guidance to relative stakeholders for future large-scale renewable energy installations in urban areas. Moreover, the proposed time-of-use grid penalty cost model provides significant references to achieve the power grid resilience and economy for large-scale renewable energy system deployment in urban communities.

Nomenclature

Acronyms	
FiT	feed-in tariff
FSOC	fractional state of charge
HV	hydrogen vehicle

LCR	load cover ratio
NPV	net present value
NSGA	Non-dominated Sorting Genetic Algorithm
PC	penalty cost
PEMFC	proton exchange membrane fuel cell
PV	photovoltaic
RE	renewable energy
SCR	self-consumption ratio
TOU	time-of-use
WT	wind turbine

List of symbols

$E_{battery\ to\ load}$	energy from battery to load, kWh
$E_{FCs\ to\ load}$	energy from fuel cells to load, kWh
E_{load}	total electrical load, kWh
E_{RE}	total renewable energy generation, kWh
$E_{RE\ to\ battery}$	energy from renewable sources to battery, kWh
$E_{RE\ to\ electrolyzer}$	energy from renewable sources to electrolyzer, kWh
$E_{RE\ to\ load}$	energy from renewable sources to load, kWh
$P_{export\_estimated}$	grid exported power estimation, kW
$P_{export\_offpeak}$	grid exported power of off-peak time, kW
P_{export_onpeak}	grid exported power of on-peak time, kW
$P_{import\_estimated}$	grid imported power estimation, kW
$P_{import\_offpeak}$	grid imported power of off-peak time, kW
P_{import_onpeak}	grid imported power of on-peak time, kW
$PC_{export\_offpeak}$	penalty cost of grid exported power of off-peak time, US$
PC_{export_onpeak}	penalty cost of grid exported power of on-peak time, US$
$PC_{import\_offpeak}$	penalty cost of grid imported power of off-peak time, US$
PC_{import_onpeak}	penalty cost of grid imported power of on-peak time, US$
PC_{TOU}	time-of-use grid penalty cost, US$
$PF_{offpeak}$	penalty factor of off-peak time, US$/kWh
PF_{onpeak}	penalty factor of on-peak time, US$/kWh

Acknowledgement

The work described in this paper was financially supported by the National Key R&D Program of China: Research and integrated demonstration on suitable technology of net zero energy building (Project No.: 2019YFE0100300). Appreciation is also given to Open University of Hong Kong Research Grant (No. 2020/1.3).

References

[1] International Energy Agency. 2019 global status report for buildings and construction: towards a zero-emissions, efficient and resilient buildings and construction sector. 2019.
[2] Environment Bureau. Hong Kong's Climate Action Plan 2030+. 2017.
[3] International Energy Agency. GlobalABC roadmap for buildings and construction 2020-2050: towards a zero-emission, efficient, and resilient buildings and construction sector. 2020.
[4] Javed MS, Zhong D, Ma T, Song A, Ahmed S. Hybrid pumped hydro and battery storage for renewable energy based power supply system. Applied Energy. 2020;257:114026.
[5] Zhou Y, Cao S. Coordinated multi-criteria framework for cycling aging-based battery storage management strategies for positive building–vehicle system with renewable depreciation: Life-cycle based techno-economic feasibility study. Energy Conversion and Management. 2020;226:113473.
[6] Zhou Y, Cao S, Hensen JLM, Lund PD. Energy integration and interaction between buildings and vehicles: A state-of-the-art review. Renewable and Sustainable Energy Reviews. 2019;114:109337.
[7] Yan J, Yang Y, Campana PE, He J. City-level analysis of subsidy-free solar photovoltaic electricity price, profits and grid parity in China. Nature Energy. 2019;4:709-17.
[8] REN 21. Renewables 2020 global status report. 2020.
[9] Hydrogen Council. Hydrogen scaling up. A sustainable pathway for the global energy transition. 2017.
[10] International Energy Agency. The future of hydrogen: seizing today's opportunities. 2019.
[11] Liu J, Chen X, Cao S, Yang H. Overview on hybrid solar photovoltaic-electrical energy storage technologies for power supply to buildings. Energy Conversion and Management. 2019;187:103-21.
[12] REN 21. Renewables in cities: 2019 global status report. 2019.
[13] International Institute for Sustainable Development SDG Knowledge Hub. 77 countries, 100+ cities commit to net zero carbon emissions by 2050 at Climate Summit. 2019.
[14] International Institute for Sustainable Development SDG Knowledge Hub. European Commission launches green deal to reset economic growth for carbon neutrality. 2019.
[15] World Resources Institute. Zero carbon buildings for all initiative launched at UN Climate Action Summit. 2019.
[16] Xinhua News. Xi Focus: Xi announces China aims to achieve carbon neutrality before 2060. 2020.
[17] The World Bank. 2019. Year in review: 2019 in 14 charts.
[18] Silverman RE, Flores RJ, Brouwer J. Energy and economic assessment of distributed renewable gas and electricity generation in a small disadvantaged urban community. Applied Energy. 2020;280:115974.
[19] Bartolini A, Carducci F, Muñoz CB, Comodi G. Energy storage and multi energy systems in local energy communities with high renewable energy penetration. Renewable Energy. 2020;159:595-609.
[20] Avilés A C, Oliva H S, Watts D. Single-dwelling and community renewable microgrids: Optimal sizing and energy management for new business models. Applied Energy. 2019;254:113665.
[21] You C, Kim J. Optimal design and global sensitivity analysis of a 100% renewable energy sources based smart energy network for electrified and hydrogen cities. Energy Conversion and Management. 2020;223:113252.
[22] Yan B, Di Somma M, Graditi G, Luh PB. Markovian-based stochastic operation optimization of multiple distributed energy systems with renewables in a local energy community. Electric Power Systems Research. 2020;186:106364.
[23] Seck GS, Krakowski V, Assoumou E, Maïzi N, Mazauric V. Embedding power system's reliability within a long-term Energy System Optimization Model: Linking high renewable energy integration and future grid stability for France by 2050. Applied Energy. 2020;257:114037.
[24] Takeshita T, Aki H, Kawajiri K, Ishida M. Assessment of utilization of combined heat and power systems to provide grid flexibility alongside variable renewable energy systems. Energy. 2021;214:118951.

[25] Mayyas A, Wei M, Levis G. Hydrogen as a long-term, large-scale energy storage solution when coupled with renewable energy sources or grids with dynamic electricity pricing schemes. International Journal of Hydrogen Energy. 2020;45:16311-25.
[26] Abdelshafy AM, Jurasz J, Hassan H, Mohamed AM. Optimized energy management strategy for grid connected double storage (pumped storage-battery) system powered by renewable energy resources. Energy. 2020;192:116615.
[27] Gharibi M, Askarzadeh A. Size and power exchange optimization of a grid-connected diesel generator-photovoltaic-fuel cell hybrid energy system considering reliability, cost and renewability. International Journal of Hydrogen Energy. 2019;44:25428-41.
[28] Allard S, Mima S, Debusschere V, Quoc TT, Criqui P, Hadjsaid N. European transmission grid expansion as a flexibility option in a scenario of large scale variable renewable energies integration. Energy Economics. 2020;87:104733.
[29] The University of Wisconsin Madison. TRNSYS 18. 2017.
[30] Hong Kong Housing Authority. Standard block typical floor plans. 2016.
[31] Qin H, Pan W. Energy use of subtropical high-rise public residential buildings and impacts of energy saving measures. Journal of Cleaner Production. 2020;254:120041.
[32] Hong Kong Electrical and Mechanical Services Department. Guidelines on Performance-based Building Energy Code. 2007.
[33] Hong Kong Building Environmental Assessment Method Society. An envrionmental assessment for new buildings Version 4/04. 2004.
[34] Liu J, Cao S, Chen X, Yang H, Peng J. Energy planning of renewable applications in high-rise residential buildings integrating battery and hydrogen vehicle storage. Applied Energy. 2021;281:116038.
[35] Solar Energy Laboratory Univ. of Wisconsin-Madison. TRNSYS 18 a transient system simulation program, Volume 4 mathematical reference. 2017.
[36] Wind turbine models. Hummer H21.0-100kW. 2017.
[37] Liu J, Chen X, Yang H, Li Y. Energy storage and management system design optimization for a photovoltaic integrated low-energy building. Energy. 2020;190:116424.
[38] Wang D, Cao X. Impacts of the built environment on activity-travel behavior: Are there differences between public and private housing residents in Hong Kong? Transportation Research Part A: Policy and Practice. 2017;103:25-35.
[39] Transport Department. The annual traffic census. 2018.
[40] Toyota USA NEWSROOM. Toyota Mirai product information. 2019.
[41] Cao S, Alanne K. Technical feasibility of a hybrid on-site H2 and renewable energy system for a zero-energy building with a H2 vehicle. Applied Energy. 2015;158:568-83.
[42] China Light and Power Hong Kong Limited. Tariff and charges. 2020.
[43] China Light and Power Hong Kong Limited. Large power tariff. 2020.
[44] Zhang Y, Jankovic L. An Interactive Optimisation Engine for Building Energy Performance Simulation. 2017.
[45] Magnier L, Haghighat F. Multiobjective optimization of building design using TRNSYS simulations, genetic algorithm, and Artificial Neural Network. Building and Environment. 2010;45:739-46.
[46] Chen X, Yang H, Zhang W. Simulation-based approach to optimize passively designed buildings: A case study on a typical architectural form in hot and humid climates. Renewable and Sustainable Energy Reviews. 2018;82:1712-25.
[47] Lee U, Park S, Lee I. Robust design optimization (RDO) of thermoelectric generator system using non-dominated sorting genetic algorithm II (NSGA-II). Energy. 2020;196:117090.
[48] Bingham RD, Agelin-Chaab M, Rosen MA. Whole building optimization of a residential home with PV and battery storage in The Bahamas. Renewable Energy. 2019;132:1088-103.
[49] International Renewable Energy Agency. Renewable power generation costs in 2017. 2018.

[50] Liu J, Wang M, Peng J, Chen X, Cao S, Yang H. Techno-economic design optimization of hybrid renewable energy applications for high-rise residential buildings. Energy Conversion and Management. 2020;213:112868.
[51] Javed MS, Ma T, Jurasz J, Canales FA, Lin S, Ahmed S, et al. Economic analysis and optimization of a renewable energy based power supply system with different energy storages for a remote island. Renewable Energy. 2021;164:1376-94.
[52] Killer M, Farrokhseresht M, Paterakis NG. Implementation of large-scale Li-ion battery energy storage systems within the EMEA region. Applied Energy. 2020;260:114166.
[53] GlobalData. Further falling inverter prices - market value declining. 2018.
[54] Assaf J, Shabani B. Transient simulation modelling and energy performance of a standalone solar-hydrogen combined heat and power system integrated with solar-thermal collectors. Applied Energy. 2016;178:66-77.
[55] Akhtari MR, Baneshi M. Techno-economic assessment and optimization of a hybrid renewable co-supply of electricity, heat and hydrogen system to enhance performance by recovering excess electricity for a large energy consumer. Energy Conversion and Management. 2019;188:131-41.
[56] Cao S, Alanne K. The techno-economic analysis of a hybrid zero-emission building system integrated with a commercial-scale zero-emission hydrogen vehicle. Applied Energy. 2018;211:639-61.
[57] Gökçek M, Kale C. Techno-economical evaluation of a hydrogen refuelling station powered by Wind-PV hybrid power system: A case study for İzmir-Çeşme. International Journal of Hydrogen Energy. 2018;43:10615-25.
[58] Jafari M, Armaghan D, Seyed Mahmoudi SM, Chitsaz A. Thermoeconomic analysis of a standalone solar hydrogen system with hybrid energy storage. International Journal of Hydrogen Energy. 2019;44:19614-27.
[59] Baldwin D. Development of high pressure hydrogen storage tank for storage and gaseous truck delivery. Hexagon Lincoln LLC, Lincoln, NE (United States); 2017.
[60] Toyota Motor Sales. 2019 Mirai fuel cell electric vehicle. 2020.
[61] Kim I, Kim J, Lee J. Dynamic analysis of well-to-wheel electric and hydrogen vehicles greenhouse gas emissions: Focusing on consumer preferences and power mix changes in South Korea. Applied Energy. 2020;260:114281.
[62] Electrical and Mechanical Services Department. Introduction to feed-in tariff of renewable energy in Hong Kong. 2018.
[63] Campbell M, Aschenbrenner P, Blunden J, Smeloff E, Wright S. The drivers of the levelized cost of electricity for utility-scale photovoltaics. White paper: SunPower corporation. 2008.
[64] Li J, Zhang X, Zhou X, Lu L. Reliability assessment of wind turbine bearing based on the degradation-Hidden-Markov model. Renewable Energy. 2019;132:1076-87.
[65] Cao S. The impact of electric vehicles and mobile boundary expansions on the realization of zero-emission office buildings. Applied Energy. 2019;251:113347.
[66] Ricke K, Drouet L, Caldeira K, Tavoni M. Country-level social cost of carbon. Nature Climate Change. 2018;8:895-900.
[67] California fuel cell partnership. Cost to refill. 2019.